CCFE
CULHAM CENTRE FOR FUSION ENERGY

UK Atomic Energy Authority

UKAEA-CCFE-PR(20)102

Yuling He, Yueqiang Liu, Xu Yang, Guoliang Xia, Li Li

Active control of resistive wall mode via modification of external tearing index

Enquiries about copyright and reproduction should in the first instance be addressed to the UKAEA Publications Officer, Culham Science Centre, Building K1/0/83 Abingdon, Oxfordshire, OX14 3DB, UK. The United Kingdom Atomic Energy Authority is the copyright holder.

The contents of this document and all other UKAEA Preprints, Reports and Conference Papers are available to view online free at scientific-publications.ukaea.uk/

Active control of resistive wall mode via modification of external tearing index

Yuling He, Yueqiang Liu, Xu Yang, Guoliang Xia, Li Li

This is a preprint of a paper submitted for publication in
Physics of Plasmas

Active control of resistive wall mode via modification of external tearing index

Yuling He[1], Yueqiang Liu[2], Xu Yang[3], Guoliang Xia[4] and Li Li[5]

[1]*Guangdong Provincial Key Laboratory of Quantum Engineering and Quantum Materials, School of Physics and Telecommunication Engineering, South China Normal University, Guangzhou 510006, China*

[2]*General Atomics, PO Box 85608, San Diego, CA 92186-5608, United States of America*

[3]*Chongqing Engineering Laboratory for Detection, Control and Integrated System, Chongqing Technology and Business University, Chongqing 400067, China*

[4]*CCFE, Culham Science Centre, Abingdon, OX14 3DB, United Kingdom of Great Britain and Northern Ireland*

[5]*College of Science, Donghua University, Shanghai 201620, China*

E-mail: heyl@m.scnu.edu.cn

Abstract: Modification of the external tearing index, $\Delta'_{\rm ext}$, by magnetic feedback is analytically investigated, for the purpose of controlling the resistive plasma resistive wall mode (RP-RWM). The matching method is pursued, by deriving expressions for the close-loop $\Delta'_{\rm ext}$ and by linking it to the counterpart from the inner layer. Various feedback coil configurations are found to generally reduce $\Delta'_{\rm ext}$ and stabilize the RWM, with either proportional or derivative control. Feedback modification of $\Delta'_{\rm ext}$ is found to be generally independent of the inner layer resistive interchange index D_R, confirming that feedback action primarily modifies the solution in the outer ideal region for the RP-RWM. Exception occurs when either the inner layer favorable curvature effect becomes sufficiently large or the feedback action is sufficiently strong to introduce a rotating RP-RWM in the static plasma, leading to

complex-valued close-loop Δ'_{ext}. The perturbed magnetic energy dissipation in the outer region, associated with the eddy current in the resistive wall, is identified as the key physics reason for feedback induced complex Δ'_{ext}. Similar results are also obtained for active control of the external kink instability, whose open-loop growth rate is significantly reduced by inclusion of the plasma resistivity. Within single poloidal harmonic approximation, which is most suitable for the matching approach, external active coils combined with poloidal sensors are often found to be more efficient for feedback stabilization of the mode at large proportional gain values. This counter-intuitive result is explained as lack of (non-resonant) poloidal harmonics for proper description of the feedback coil geometry.

I. Introduction

Magneto-hydrodynamic (MHD) instabilities, such as the external kinks (EK) and (neoclassical) tearing modes (TM), are major concerns for high pressure advanced tokamaks (AT).[1] Within certain pressure limit, the EK can be stabilized by a perfectly conducting wall located sufficiently close to the plasma edge.[2] However, the wall has finite conductivity in reality, which allows the leakage of the radial magnetic flux perturbation through the wall at long time scale. The resulting residual instability is called the resistive wall mode (RWM). The RWM often limits the operational space

of advanced tokamaks, because such a low- n (n is the toroidal mode number) macroscopic instability sets a beta limit[3] for the AT operation. In order to maximize the benefit of the AT scenario, such as that foreseen in ITER,[1] the RWM needs to be stabilized.

Numerical and analytical calculations,[4-9] based on the ideal MHD model, indicate that stabilization of the ideal plasma RWM (IP-RWM) can be achieved by certain free energy dissipation mechanism(s) inside the plasma in the presence of toroidal plasma rotation. The critical rotation frequency for a complete stabilization of the mode was predicted to be several percent of the Alfven frequency. However, early work[10-12] employing the resistive MHD model showed that the toroidal curvature effect, associated with the resistive layer near the rational surfaces, can stabilize the resistive-plasma RWM (RP-RWM), though with the stability window being narrow in toroidal geometry. More recent studies indicated that a slow plasma rotation flow, with the flow speed several times larger than the typical tearing mode growth rate, in combination with the resistivity layer induced energy dissipation, can stabilize the RP-RWM.[13-15]

Plasmas in future reactors are expected to rotate with low or negligible speed. Therefore, active control of the plasma instability in the absence of flow is of particular interest. Active control of the RWM has been studied for both resistive and ideal plasma models,[16-21] showing that

a magnetic feedback system, combined with the slow plasma flow, can stabilize the mode. Finn[22] studied direct feedback stabilization of the resistive plasma (tearing-like) modes utilizing magnetic coils. It was found that, in the linear phase, the growth rate of the mode can be feedback stabilized even when the plasma pressure exceeds the ideal wall limit.

In analytic theory, active control of the RWM is often studied relying on the plasma response model (PRM),[23-25] which is suitable for studying feedback control of the IP-RWM. In contrast, study of the RP-RWM is conventionally analyzed by proper matching procedures.[26] The matching approach is similar to the analysis employed for studying the TM, by separately solving the MHD equations in the inner resistive layer and in the outer ideal bulk region.[27] The matching condition often involves a key parameter Δ' (the tearing index) from both the internal and external solutions. The external tearing index, Δ'_{ext}, is defined as the logarithmic derivative jump of the perturbed radial magnetic field across the mode resonant surface (or the ratio of small to large solutions in general cases). A recent study has shown that this tearing index can be modified by a simple magnetic feedback,[28] without considering the role played by the resistive wall. The external tearing index is matched to that from the resistive layer solution to obtain the final dispersion relation for the RP-RWM. It is expected that stability of the RP-RWM can be modified

by actively controlling the external tearing mode index Δ'_{ext} - a venue pursued in this work.

In this work, we carry out analytic study of feedback stabilization of the RWM via the matching approach, based on a cylindrical plasma model. We investigate feedback modification of Δ'_{ext}, while systematically considering two choices of controllers: the proportional (P) and proportional-derivative (PD) controllers. Although the focus of this work is on the RWM, the approach exploited here is also applicable for controlling stability of the tearing mode.

In Sec. II, we present the details of our analytic model on feedback modification of Δ'_{ext} by the P- and PD-control. In Sec. III, we investigate feedback stabilization of the IP-RWM via modification of Δ'_{ext}, and compare the results with that from the PRM approach. Based on the matching approach, Sec. IV reports feedback study for the RP-RWM with or without the favorable average curvature effect (i.e. the GGJ effect discovered by Glasser, Green and Johnson[29]). Inspired by Finn's work,[22] we also carry out a similar study on the resistive plasma external kink (RP-EK) mode, following the matching approach in Sec. V. Section VI draws conclusions.

II. Analytic model

Our analytic model is based on a cylindrical circular plasma. In what

follows, we start by describing the open-loop model, followed by the closed-loop model with the P-control and finished by introducing the PD-control.

A. Open-loop model

In the cylindrical geometry, we consider the well-known Newcomb equation with finite plasma pressure in the outer region[30]

$$-\frac{\gamma^2}{F}\nabla_\perp\cdot\left(\rho\nabla_\perp\frac{\psi}{F}\right)=\frac{1}{r}\frac{d}{dr}\left(r\frac{d\psi}{dr}\right)-\frac{m^2}{r^2}\psi-\frac{m}{rF}\frac{dJ_z}{dr}\psi-\frac{2m^2B_\theta^2}{r^3B_z^2F^2}\frac{dP}{dr}\psi \quad (1)$$

where r and θ are the radial coordinate and the poloidal angle of the plasma cross section, respectively. J_z is the plasma equilibrium density along the cylinder and P is the equilibrium pressure. γ is the eigenvalue of the instability (the RWM in our case). ψ is the m-th poloidal harmonic of the perturbed poloidal magnetic flux function, which has an $\exp(im\theta - ikz)=\exp(im\theta - in\phi)$ variation, where $k=n/R_0$ with n being the toroidal mode number and R_0 the equivalent major radius. $F\equiv mB_\theta - kB_z$, with $\mathbf{B}=B_\theta\hat{\theta}+B_z\hat{z}$ being the equilibrium field.

Simplified equilibrium radial profiles are assumed, as shown in Fig. 1. The equilibrium current density $J_z(r)$ is a step function with $J_z=J_0=const$ at $0\le r<r_0$ and $J_z=0$ at $r_0<r\le a$. The plasma equilibrium pressure is assumed to be constant, $P=P_0=const$, across the whole plasma column. The toroidal equilibrium field is also assumed to be a constant. As a result, the radial profile of the safety factor, $q(r)$, is a

constant $q = q_0$ at $0 \le r < r_0$ and a parabolic function at $r_0 < r \le a$. The parameters are chosen such that only one resonant surface is present inside the plasma, for the $n = 1$ perturbation.

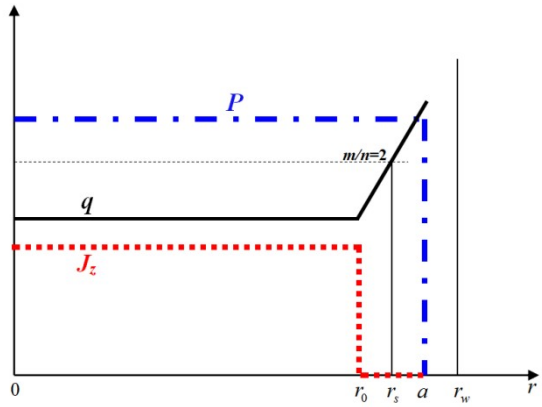

Fig. 1 The equilibrium profiles of the plasma pressure P, the axial current density J_z and the safety factor q. One rational surface $q = m/n = 2$ $(n = 1)$ is located inside the plasma.

The Laplace equation $\nabla_\perp^2 \psi \equiv 0$ is satisfied everywhere inside and outside the plasma region, except at the radial points $r = r_0, a, r_w$, where r_w denotes the resistive wall minor radius. The jump conditions for the radial derivative of the flux function ψ can be easily obtained, by integrating Eq. (1) across the above discrete radial points. We have

$$\left.\frac{r[\psi']}{\psi}\right|_{r_0} = -\frac{2m}{m - nq_0} \tag{2}$$

$$\left.\frac{r[\psi']}{\psi}\right|_{a} = -\frac{\beta m^2}{(m - nq_a)^2} \tag{3}$$

$$\left.\frac{r[\psi']}{\psi}\right|_{r_w} = \gamma\tau_w \tag{4}$$

where $\beta = 2\mu_0 P_0 / B_z^2$ is the ratio of the plasma pressure to the magnetic pressure, $q_a = q_0 (a/r_0)^2$ is the safe factor value at the plasma surface, and $\tau_w = \mu_0 r_w d_w / \eta_w$ characterizes the magnetic flux diffusion time through the resistive wall, with d_w and η_w denoting the wall thickness and resistivity, respectively.

The solution of the Laplace equation satisfies the following relation between any two discrete points r_1 and r_2, provided that the solution is smooth within the interval (r_1, r_2)

$$\frac{1+\frac{1}{m}\frac{r\psi'}{\psi}\Big|_{r_1+}}{1-\frac{1}{m}\frac{r\psi'}{\psi}\Big|_{r_1+}} = \left(\frac{r_1}{r_2}\right)^{2m} \frac{1+\frac{1}{m}\frac{r\psi'}{\psi}\Big|_{r_2-}}{1-\frac{1}{m}\frac{r\psi'}{\psi}\Big|_{r_2-}} \tag{5}$$

The above relation helps to connect different regions separated by the jump conditions (2)-(4). With the additional conditions of $r\psi'/\psi|_{r_0-} = m$ and $r\psi'/\psi|_{r_w+} = -m$, one can derive the jump of the logarithmic derivative $\Delta'_{\text{ext}} \equiv [\psi'(r_s+) - \psi'(r_s-)]/\psi(r_s)$ across the mode rational surface r_s

$$\Delta'_{\text{ext}} = -\frac{2m}{r_s}\left[\frac{B}{\alpha_s + (1-\alpha_s)B} - \frac{A}{\alpha_0 + (1-\alpha_0)A}\right] \tag{6}$$

where $B = \frac{1}{1-\alpha_w \alpha_{rw}} - \hat{\beta}$ with $\alpha_{rw} = \frac{\gamma\tau_w}{\gamma\tau_w + 2m}$, and $A = A_0 - (\gamma\tau_A)^2 A_1$ with $A_0 = \frac{1}{m - nq_0}$ and $A_1 = \frac{q_0^2}{2(m-nq_0)^2}$, with the latter often being a negligible inertia term for the RWM. The additional notations are defined as $\hat{\beta} \equiv \frac{m\beta}{2(m-nq_a)^2}$, $\alpha_w \equiv a^{2m}/r_w^{2m}$, $\alpha_s \equiv r_s^{2m}/a^{2m}$ and $\alpha_0 \equiv r_s^{2m}/r_0^{2m}$. Note that Δ'_{ext}

here is defined as the external tearing index within the so-called constant- ψ approximation. Expression (6) is the value of Δ'_{ext} in the absence of any active control. The growth rate of the open-loop IP-RWM can be obtained by setting $\Delta'_{\text{ext}} = 0$.

B. Close-loop with proportional feedback

A magnetic feedback system consists of sensor coils, active coils and control logic. We consider three types of sensors (all located at the wall radius r_w). One is the radial sensor, with the sensor signal y defined as the radial flux $\psi(r_w)$ at the wall radius. The other two, the external poloidal sensor and the internal poloidal sensor, are defined as $y = -r\psi'\big|_{r_w+}$ and $y = -r\psi'\big|_{r_w-}$, respectively. Furthermore, we consider two types of active coils, defined by their relative radial location to the wall. For the active coils located outside the wall, $r_w < r_f$, the field solution can be written as $\psi(r) = \psi_f \left(\frac{r}{r_w}\right)^m + c\left(\frac{r}{r_w}\right)^{-m}$ in the vacuum region $r_w < r < r_f$, where $\psi_f \equiv \psi_f(r_w)$ is the free-space field at the wall radius and produced by the active coil current solely. For the active coils located between the plasma surface and the wall, $a < r_f < r_w$, the field solution can be written as $\psi(r) = \alpha_f \psi_f \left(\frac{r}{r_w}\right)^m + c_1\left(\frac{r}{r_w}\right)^m + c_2\left(\frac{r}{r_w}\right)^{-m}$, with $\alpha_f \equiv r_w^{2m}/r_f^{2m}$, in the vacuum region $a < r < r_f$ and $\psi(r) = \psi_f \left(\frac{r}{r_w}\right)^{-m} + c_1\left(\frac{r}{r_w}\right)^m + c_2\left(\frac{r}{r_w}\right)^{-m}$ in the vacuum region $r_f < r < r_w$.

The simplest feedback logic is $\psi_f = -Ky$, where $K = k_P$ is the proportional feedback gain. For the external active coils, the above feedback logic, together with the wall jump condition, Eq. (4), help to relate the coefficient c to ψ_f for different types of sensors. For the internal active coils, similar relations of the coefficients c_1 and c_2 to ψ_f are obtained by employing the above feedback logic with condition $r\psi'/\psi|_{r_w+} = -m$ and the wall jump condition (4) on the perturbed field in the vacuum region $r_f < r < r_w$. This allows us to calculate the logarithmic derivative of the perturbed flux function just outside the plasma surface

$$\left.\frac{r\psi'}{\psi}\right|_{a+} = m\left[1 - \frac{2}{1-\alpha_P\, a^{2m}/r_w^{2m}}\right] \tag{7}$$

where α_P is a key quantity describing different configurations of the proportional feedback system

$$\alpha_P = \begin{cases} \dfrac{\gamma\tau_w + 2mk_P}{\gamma\tau_w + 2mk_P + 2m} & ext.coil + rad.sensor \\ \dfrac{(1-2mk_P)\gamma\tau_w + 2m^2k_P}{(1-2mk_P)\gamma\tau_w + 2m - 2m^2k_P} & ext.coil + ext.pol.sensor \\ \dfrac{\gamma\tau_w + 2m^2k_P}{\gamma\tau_w + 2m - 2m^2k_P} & ext.coil + int.pol.sensor \\ \dfrac{\gamma\tau_w + 2mk_P\alpha_f}{\gamma\tau_w + 2mk_P + 2m} & int.coil + rad.sensor \\ \dfrac{\gamma\tau_w + 2m^2k_P\alpha_f}{\gamma\tau_w + 2m + 2m^2k_P} & int.coil + ext.pol.sensor \\ \dfrac{(1+2mk_P\alpha_f)\gamma\tau_w + 2m^2k_P\alpha_f}{(1+2mk_P)\gamma\tau_w + 2m + 2m^2k_P} & int.coil + int.pol.sensor \end{cases}$$

Connecting Eqs. (2,3,7) via relation (5) across various regions, we derive the following expression for Δ'_{ext} at the rational surface r_s , in the

presence of proportional feedback control

$$\Delta'_{\mathrm{ext},P}(K,\gamma) = -\frac{2m}{r_s}\left[\frac{B_P}{\alpha_s + (1-\alpha_s)B_P} - \frac{A}{\alpha_0 + (1-\alpha_0)A}\right] \tag{8}$$

where $B_P = \frac{1}{1-\alpha_w\alpha_P} - \hat{\beta}$. Comparing the close-loop expression (8) with the open-loop expression (6), we find that feedback modifies the external tearing index only via the B_P factor. The proportional feedback gain K enters into Eq. (8) via the α_P factor. The change of Δ'_{ext} due proportional feedback is

$$\begin{aligned}\delta\Delta'_P &= \Delta'_{\mathrm{ext},P}(K,\gamma) - \Delta'_{\mathrm{ext}}(K=0,\gamma) \\ &= -\frac{2m}{r_s}\frac{(\alpha_P - \alpha_{rw})\alpha_s\alpha_w}{[C + (1-\alpha_s - C)\alpha_w\alpha_P][C + (1-\alpha_s - C)\alpha_w\alpha_{rw}]}\end{aligned} \tag{9}$$

where $C = \alpha_s + (1-\alpha_s)(1-\hat{\beta})$. We remark that the above result assumes the same growth rate between the open-loop and close-loop systems, which is generally not the case. The growth rate need to be self-consistently evaluated based on the RWM dispersion relations (with or without feedback). This will be addressed in sections III-V.

C. Close-loop with proportional-derivative feedback

Now we consider PD feedback with the control logic of $\psi_f = -[k_P + sk_D]y$, where k_D is the derivative gain and s is the eigenvalue of the close-loop system. Following a similar procedure to that outlined for the P-controller, we arrive at the following expression for the external tearing index in the presence of PD-feedback

$$\Delta'_{\mathrm{ext},PD}(K,\gamma) = -\frac{2m}{r_s}\left[\frac{B_{PD}}{\alpha_s + (1-\alpha_s)B_{PD}} - \frac{A}{\alpha_0 + (1-\alpha_0)A}\right], \tag{10}$$

where $B_{PD} = \dfrac{1}{1-\alpha_w\alpha_{PD}} - \hat{\beta}$ and

$$\alpha_{PD} = \begin{cases} \dfrac{\gamma\tau_w(1+2mk_D)+2mk_P}{\gamma\tau_w(1+2mk_D)+2mk_P+2m} & ext.coil + rad.sensor \\[2ex] \dfrac{\gamma\tau_w(1-2mk_P+2m^2k_D)+2m^2k_P-2mk_D(\gamma\tau_w)^2}{\gamma\tau_w(1-2mk_p-2m^2k_D)+2m-2m^2k_P-2mk_D(\gamma\tau_w)^2} & ext.coil + ext.pol.sensor \\[2ex] \dfrac{\gamma\tau_w(1+2m^2k_D)+2m^2k_P}{\gamma\tau_w(1-2m^2k_D)-2m^2k_P+2m} & ext.coil + int.pol.sensor \\[2ex] \dfrac{\gamma\tau_w(1+k_D\alpha_f)+2mk_P\alpha_f}{\gamma\tau_w(1+2mk_D)+2mk_P+2m} & int.coil + rad.sensor \\[2ex] \dfrac{\gamma\tau_w(1+2m^2k_D\alpha_f)+2m^2k_P\alpha_f}{\gamma\tau_w(1+2m^2k_D)+2m^2k_P+2m} & int.coil + ext.pol.sensor \\[2ex] \dfrac{\gamma\tau_w(1+2mk_P\alpha_f+2m^2k_D\alpha_f)+2m^2k_P\alpha_f+2mk_D\alpha_f(\gamma\tau_w)^2}{\gamma\tau_w(1+2mk_P+2m^2k_D)+2m+2m^2k_P+2mk_D(\gamma\tau_w)^2} & int.coil + int.pol.sensor \end{cases}$$

The change of Δ'_{ext}, due to PD-control, becomes

$$\begin{aligned} \delta\Delta'_{PD} &= \Delta'_{\mathrm{ext},PD}(K,\gamma) - \Delta'_{\mathrm{ext}}(K=0,\gamma) \\ &= -\frac{2m}{r_s}\frac{(\alpha_{PD}-\alpha_{rw})\alpha_s\alpha_w}{[C+(1-\alpha_s-C)\alpha_w\alpha_{PD}][C+(1-\alpha_s-C)\alpha_w\alpha_{rw}]} \end{aligned} \tag{11}$$

where the constant C is the same as that from Eq. (9).

D. Inner layer solutions

Expressions (6,8,10) depend on the mode eigenvalue γ, which is *a-priori* unknown. The only case, where the value of Δ'_{ext} can be explicitly calculated, is when the wall time vanishes (i.e. in the absence of the resistive wall). This was the case considered in Ref. [28]. In more general

cases, we need to solve the dispersion relation for the RWM, by setting the external tearing index to zero (for the IP-RWM) or by matching the external and internal solutions (for the RP-RWM), in order to find the mode eigenvalue γ.

For a pressureless plasma (i.e. $\beta = 0$) without the GGJ effect, the inner tearing index at the resonant surface is conveniently written as[31]

$$\Delta'_{\text{int}}(\gamma) = 2.12(ns)^{-1/2} S^{3/4} (\gamma\tau_A)^{5/4}, \tag{12}$$

where s is the magnetic shear (at the mode rational surface) and S the Lundquist number. For a plasma with finite equilibrium pressure (and pressure gradient) at the rational surface, it is helpful to consider the GGJ effect. The inner tearing index in this case takes the form[32-33]

$$\Delta'_{\text{int}}(\gamma) = 2.12 A_s (\gamma\tau_A)^{5/4} \left[1 - \frac{\pi}{4} D_R B_s (\gamma\tau_A)^{-3/2} \right], \tag{13}$$

where $A_s = (ns)^{-1/2} (1 + 2q_{r_s}^2)^{1/4} S^{3/4}$ and $B_s = (ns)(1 + 2q_{r_s}^2)^{-1/2} S^{-1/2}$. D_R is the resistive interchange index, which is roughly proportional to the plasma pressure at the rational surface. Note that D_R is typically a small negative number for tokamak plasmas, which we shall treat as a free parameter in our analytic model. We emphasize that, for a given plasma equilibrium, the D_R value is fixed. Therefore, treating D_R as a free parameter introduces in-consistency in the model, which on the other hand has minor consequences on our main conclusions reported later on. Treating D_R as a free parameter allows us to examine the effect of the strength of the GGJ effect on the RP-RWM.

Knowing the analytic forms for both the inner and outer tearing indices, the matching condition

$$\Delta'_{\text{ext}}(K,\gamma)=\Delta'_{\text{int}}(\gamma) \tag{14}$$

then leads to the dispersion relation for the RP-RWM, in the presence of magnetic feedback.

Since the above dispersion relation involves the eigenvalue γ in a non-liner manner, we shall provide numerical solutions in the following sections III-V. We then insert the calculated γ value into the external tearing index, in order to find out how the magnetic feedback modifies the tearing index. We perform the study for the IP-RWM (Sec. III), RP-RWM (Sec. IV) and RP-EK (Sec. V), respectively. For each type of instability, we shall consider P- and PD-control schemes, utilizing Eqs. (8) and (10), respectively. In this study, we neglect the integral control action which mainly shapes the control performance (e.g. reduces the settling time). We leave tearing index modification by more advanced controllers to future studies.

III. Feedback control of IP-RWM

Analytic theory of active control of the IP-RWM has been well developed during past years. The previous study, however, largely relied on directly solving the coupled MHD-feedback equations,[34-35] or on the PRM.[23-25] We follow a different approach here, namely by requiring vanishing tearing

index at the resonant surface for the IP-RWM. We shall show that both the PRM approach and the matching approach yield the same feedback results.

We consider two plasma equilibria, one with vanishing plasma pressure ($\beta = 0$) and one with a finite equilibrium pressure ($\beta = 0.03$). Chosen are the following basic parameters: $a = 1$, $m = 2$, $n = 1$, $r_0 = 0.63a$, $r_s = 0.9a$ and $r_w = 1.2a$. Furthermore, we assume $r_f = 1.3a$ for the external active coil and $r_f = 1.1a$ for the internal active coil. The other parameters are also fixed: the Lundquist number $S = 5 \times 10^7$ (for the case of resistive plasma), and the wall time $\tau_w = 10^4 \tau_A$. These basic parameters are chosen to ensure a typical RWM regime.

The open-loop stability can be tuned by varying the on-axis safety factor q_0. One example with $\beta = 0$ is shown in Fig. 2. The growth rate here is obtained by solving the dispersion relation $\Delta'_{\text{ext}} = 0$ for the ideal plasma and Eq. (14) for the resistive plasma, but at feedback gain $K = 0$. Note that the inertial term, associated with the A_1 factor (cf. expression (6)), has been retained in solving the aforementioned dispersion relations. It is important to include this inertial factor in order to recover the ideal-plasma external kink (IP-EK) and the RP-EK regimes shown in Fig. 2. With our parameter setting, transition from the RWM regime to the EK regime occurs at $q_0 = 1.076$ (vertical dashed line in Fig. 2). This threshold q_0 value is determined by $1 - (m - nq_0) - (r_0/r_w)^{2m} = 0$ (Appendix A). The

EK regime corresponds to $1-(m-nq_0)-(r_0/r_w)^{2m}>0$ at $q_0>1.076$, and the RWM regime corresponds to $1-(m-nq_0)-(r_0/r_w)^{2m}<0$ at $q_0<1.076$. The aforementioned inertial term is negligible for the RWM regime.

Note that Fig. 2 also compares the mode stability between ideal and resistive plasma assumptions. Inclusion of the plasma resistivity is found to substantially reduce the growth rate of the RWM (as well as that of the EK to large extent). This agrees with our previous finding,[13-14] although the latter was obtained via a completely different approach (i.e. the extended energy principle approach for the open-loop RWM). The relatively small growth rate for the three instabilities, i.e. the IP-RWM, RP-RWM and RP-EK, implies that active magnetic control (with practically reasonable control response time) can be applied to stabilize these modes. This is precisely the subject of the following studies.

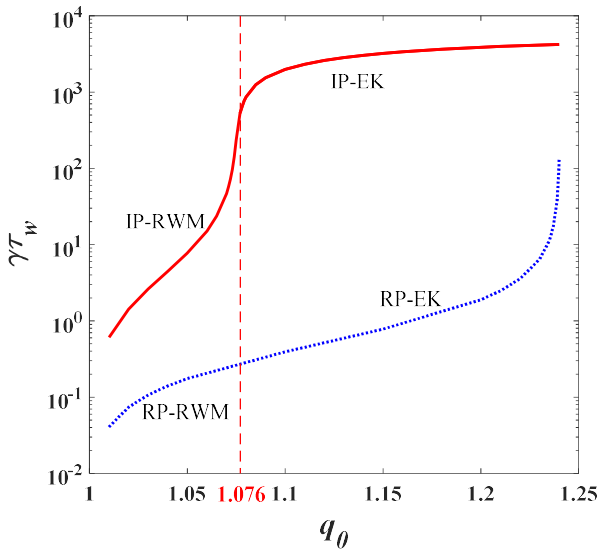

Fig. 2 The open-loop growth rate of the n=1 instability in different regimes while scanning the on-axis safety factor q_0: the ideal plasma resistive wall mode (IP-RWM), the ideal plasma external kink (IP-EK), the resistive plasma resistive wall mode

(RP-RWM), and the resistive plasma external kink (RP-EK). The vertical dashed line indicates the transition value ($q_0 = 1.076$) from the RWM regime to the EK regime. The other equilibrium parameter is $\beta = 0$.

A. Control of IP-RWM with P-feedback

Now we numerically solve the close-loop dispersion relation $\Delta'_{\mathrm{ext},P}(K,\gamma) = 0$ (i.e. expression (8) $= 0$) in the presence of a P-controller. The results are plotted in Fig. 3 while scanning the proportional feedback gain $K = k_P$. Compared are the growth rates of the IP-RWM in a plasma with vanishing equilibrium pressure $\beta = 0$ (Fig. 3(a)) and with finite equilibrium pressure $\beta = 0.03$ (Fig. 3(b)). Six combinations of the active and sensor coil types are considered as indicated in the figure.

Proportional feedback can stabilize the IP-RWM, either with or without pressure, when the proportional gain achieves certain critical value. This holds for all six feedback coil configurations. The stabilizing effect with internal active coils is stronger than that with external active coils at small feedback gain, independent of the choice of the sensor type (but assuming the same sensor type). At large gain values and with (either internal or external) poloidal sensors, however, feedback with external active coils outperforms that with internal active coils. In fact, we find similar results also for RP-RWM and RP-EK as will be reported later on.

The above finding appears to be counter-intuitive. The expectation is that, with the same type of sensor coils, placing the active coils inside the

resistive wall should always be better than placing them outside the wall, by two reasons. First, the control field is stronger since the internal active coil is closer to the plasma. Secondly, with the internal active coils, the control field does not need to penetrate through the resistive wall in order to reach the plasma. We remark that the second argument does not apply to the case of marginal stability (assuming that the marginal stability is reached at vanishing mode frequency), since the wall eddy current vanishes in this case. But the first argument always applies.

It turns out that this counter-intuitive behavior is the result of the single harmonic approximation that we adopt in this study. The single harmonic approximation is a natural choice for the matching approach (as well as for the cylindrical plasma). Note that the equilibrium that we choose has only a single resonant harmonic $m/n = 2/1$. The multi-harmonic coupling effect thus can only come from the non-resonant harmonics and is a feedback coil geometry effect.

To illustrate this, we return to the PRM approach (Appendix B). The latter allows us to include all the poloidal Fourier harmonics into the plasma response transfer function, despite the fact that the $2/1$ mode is the only unstable mode in the spectrum. Inclusion of all poloidal harmonics is needed primarily to properly describe the feedback coil geometry,[23] which is where our intuition develops from. In other words, window-pane active coils and point-wise poloidal sensor signals require

many poloidal harmonics to resolve. As soon as we add all the other (non-resonant) harmonics (associated with stable RWM) into the PRM, we find that the internal active coils always outperform the external counterpart (Fig. B(c), Appendix B).

Even more interestingly, it turns out that the major role in resolving the puzzle is played by the m=-2 harmonic. By only including the $m = \pm 2$ contributions into the PRM, the aforementioned counter-intuitive phenomenon also disappears (Fig. B(b), Appendix B). The fundamental reason here is a cancellation effect between the +m and -m harmonics as discovered in Ref. [25].

As mentioned before, it is unfortunately not straightforward to include multiple harmonics (in particular that of the non-resonant sideband) into the matching approach. [The PRM approach as developed in Refs. [24-26] is suitable for including multiple harmonics but is not suitable for including the resistive layer physics.] Therefore, caution need to be taken when discussing the feedback results (in particular that with the external active coils and poloidal sensors) predicted by the matching approach with single harmonic approximation, which does not properly describe the realistic feedback coil geometry as adopted in experiments.

As a final remark to the results shown in Fig. 3, we notice that the open-loop growth rate is about twice larger for the plasma with finite equilibrium pressure ($\beta = 0.03$, Fig. 3(b)). The critical gain required for full

stabilization of the IP-RWM is also larger.

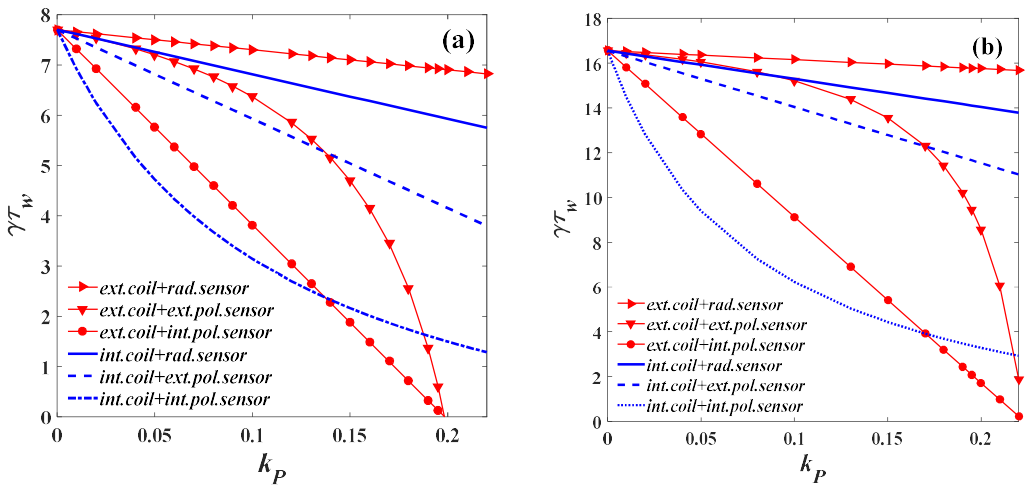

Fig. 3 The growth rate of the n=1 IP-RWM versus the proportional feedback gain value k_P, assuming various combinations of the active and sensor coil types and (a) vanishing equilibrium pressure $\beta = 0$, (b) finite equilibrium pressure $\beta = 0.03$. The on-axis safety factor is fixed at $q_0 = 1.05$.

B. Control of IP-RWM with PD-feedback

Now we consider a PD-controller. We shall vary the derivative gain k_D at fixed proportional gain of $k_P = 0.1$. We again numerically solve the IP-RWM dispersion relation $\Delta'_{\text{ext},PD}(K,\gamma) = 0$ (i.e. expression (10) $= 0$) but with PD-feedback. The results are reported in Fig. 4, again assuming various combinations of the active and sensor coil types. For both plasmas (with vanishing or finite equilibrium pressure), the derivative action reduces the mode growth rate, except the case of internal active coil combined with the radial sensor. The latter, somewhat surprising,

result can be analytically understood. For this specific case, the growth rate of the close-loop system becomes $\gamma\tau_w = (-C_3 k_P + C_1)/(-C_4 k_D + 1)$ with vanishing equilibrium pressure $\beta = 0$ (Eq. (A.3), Appendix A). At fixed proportional gain of $k_P = 0.1$, the numerator $-C_3 k_P + C_1 > 0$. Since $C_4 > 0$, increasing derivative gain (up to certain limit) also increases the mode growth rate.

We note that the IP-RWM cannot be fully stabilized by the derivative action. At fixed proportional gain, the mode growth rate approaches a positive constant at infinity derivative gain. This is understandable, since the stabilizing effect of the derivative action diminishes as the mode approaches the marginal stability point (at vanishing mode frequency).

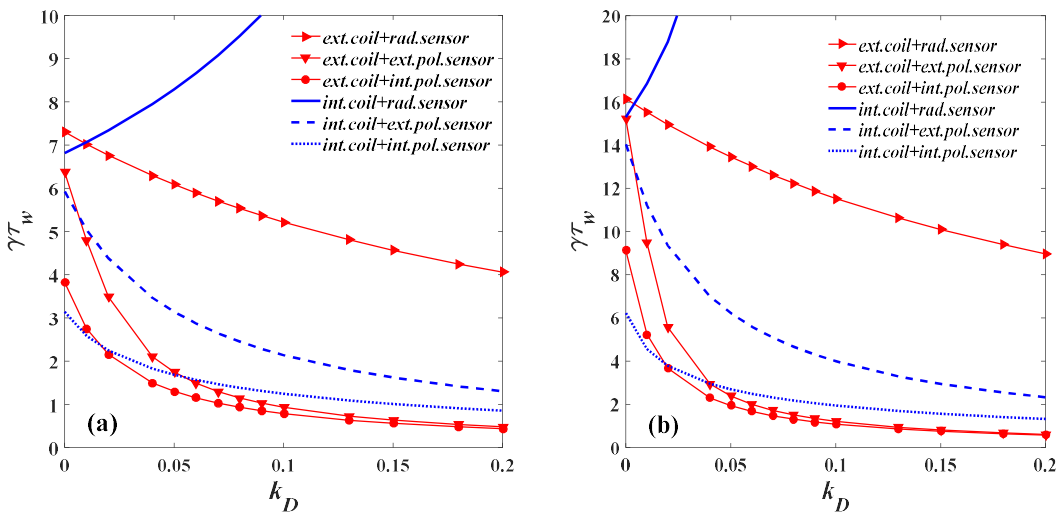

Fig. 4 The growth rate of the n=1 IP-RWM versus the derivative gain, assuming various combinations of the active and sensor coil types. The proportional feedback gain is fixed at $k_P = 0.1$. Considered are two equilibria with either (a) vanishing pressure $\beta = 0$ or (b) finite pressure $\beta = 0.03$. The on-axis safety factor is fixed at $q_0 = 1.05$.

IV. Feedback control of RP-RWM via modification of Δ'_{ext}

If the IP-RWM feedback study presented in Sec. III can be carried out with either the PRM or matching approach, the latter is much more suitable for studying feedback control of the RP-RWM. Even more interestingly, the matching approach allows us to quantify the effect of magnetic feedback on the tearing index Δ'_{ext}. In what follows, we demonstrate that feedback indeed modifies Δ'_{ext}. Moreover, we show that feedback modification of the external tearing index does not depend on the inner layer physics, i.e. on variation of the D_R value. The basic plasma parameters (except those in the resistive layer) are assumed the same as that from Sec. III.

A. Feedback with proportional gain

With proportional control, stability of the close-loop for the RP-RWM is determined by solving the dispersion relation (14) which links Eq. (8) with Eq. (12) or (13), depending on whether the GGJ effect is included into the layer model. As mentioned before, we include the GGJ physics (Eq. (13)) into the inner layer for the equilibrium with finite pressure. The feedback results for both equilibria (with vanishing or finite pressure) are summarized in Fig. 5. Similar to results reported in Sec. III for the IP-RWM, proportional feedback reduces the growth rate of the RP-RWM, with all six feedback coil configurations considered in this work. The

combination of internal active coils with internal poloidal sensor performs the best at low feedback gain. At higher feedback gain, we again obtain the counter-intuitive result of the superior performance by the external active coils. Since the behavior is qualitatively similar to that of the IP-RWM, we expect that the same reasoning (i.e. the single harmonic approximation versus the requirement of multiple poloidal harmonics to correctly describe the feedback coil geometry) also applies here to explain this counter-intuitive behavior.

We now analyze some details of the results presented in Fig. 5, first focusing on the vanishing equilibrium pressure case without the GGJ effect. Figure 5(a) shows that the critical gain values for k_P, corresponding to marginal stability of the RP-RWM with the external active coils and the internal or external poloidal sensors, coincide. This is because the wall eddy current disappears at the marginal instability. Therefore, the wall is effectively in absence under this peculiar circumstance. In other words, the (normally qualitative) difference between the internal and external poloidal sensors disappears at the marginal instability point (and with vanishing mode frequency which is the case here).

Inserting the mode growth rate shown in Fig. 5(a) back into expression (8), we obtain feedback modification of the external tearing index as reported in Fig. 5(b). The overall behavior, among various

combinations of the feedback coils, resemble that of the stability plot shown in Fig. 5(a). This is understandable, since the inner tearing index in this case scales with the mode growth rate in a simple proportionality manner (Eq. (12)). Nevertheless, Fig. 5(b) convincingly demonstrates that feedback reduces the external tearing index, and by doing so, stabilizes the RP-RWM.

Next, we discuss Fig. 5(c-d) for the finite pressure equilibrium case, where the GGJ effect is included into the inner layer tearing index (Eq. (13)). The feedback results are generally similar to that without the GGJ-effect (Fig. 5(a-b)). One qualitative difference though is the appearance of complex eigenvalues (i.e. finite mode frequencies) at large proportional gains as shown in Fig. 5(c). This occurs for the close-loop with either internal or external poloidal sensors. It is known that, in the absence of feedback, the GGJ effect can introduce complex frequency to the RP-RWM even for a static equilibrium, if the D_R value is sufficiently negative.[14] In our case, however, the D_R value is chosen such that the open-loop eigenvalue is real. The finite mode frequency is thus introduced by the feedback action (but in the presence of the GGJ effect).

Figure 5(d) shows the corresponding Δ'_{ext} for the case with GGJ effect. The general trend of the proportional feedback is again to reduce Δ'_{ext}. The most interesting observation here, however, is that the

corresponding external tearing index becomes complex-valued at sufficiently large feedback gain. The imaginary part of Δ'_{ext} is small (by about three orders of magnitude in this case) compared to that of the real part, but much larger imaginary part is also obtained as will be shown in later examples. Note that complex Δ'_{ext} occurs whenever the close-loop eigenvalue becomes complex. This feature of complex Δ'_{ext} is qualitatively different from the open-loop TM theory, where sufficiently large GGJ effect introduces finite mode frequency but the tearing index remains real-valued.

Close examination of the close-loop external tearing index reveals two possible perturbed energy sources from the outer region, that can introduce complex Δ'_{ext} in the presence of a rotating close-loop RP-RWM (in the static plasma). One is the plasma inertia, while the other is the presence of a resistive wall. For the RWM, the plasma inertia (from the outer region) is known to play a minor role on the mode dynamics. In fact, in our example, the inertia term (associated with the A_1 factor, see Eq. (6)) is about $(\tau_w/\tau_A)^2 = 10^8$ times smaller than that due to the resistive wall, with the latter providing an order unity contribution to Δ'_{ext}. The major role in inducing complex-valued external tearing index is thus played by the resistive wall, which provides perturbed energy dissipation due to the wall eddy current. To further verify this conclusion, we performed feedback calculations similar to that presented in Fig. 5(c-d),

but this time assuming $\tau_w = 0$ in Eq. (8). The close-loop Δ'_{ext} indeed becomes real-valued in this case, even in the presence of large feedback gain and complex RP-RWM eigenvalues.

Another interesting observation is that the real part of the external tearing index is nearly independent of the assumed D_R value when we scan the feedback gain, despite the fact that the close-loop eigenvalue substantially varies with D_R. This is illustrated in Fig. 6, where we assume a control scheme with external active coils and the internal poloidal sensor. For a given D_R value, the close-loop eigenvalue becomes complex at certain feedback gain, but the mode is still unstable (Fig. 6(a)). Further increasing feedback gain results in full stabilization of the RP-RWM, with the critical gain value (for marginal stability) increasing with increasing the amplitude of D_R. A small imaginary part (insert in Fig. 6(b)) of Δ'_{ext} again appears when the close-loop eigenvalue becomes complex. But the real part of Δ'_{ext} is almost independent of the choice for the D_R value. In other words, the results show that the magnetic feedback system modifies the external tearing index almost independent of the inner layer physics.

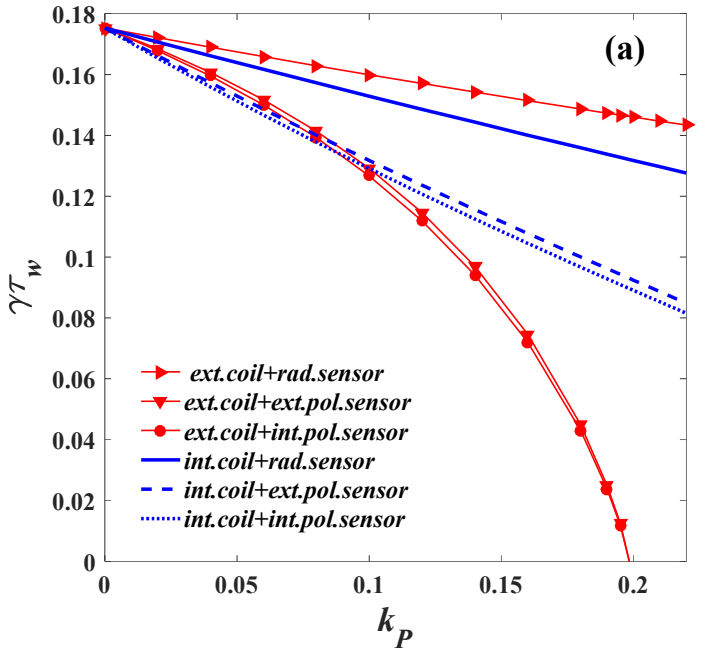
(a)
0.18
0.16
0.14
0.12
0.1
0.08
0.06
0.04
0.02
0
$\gamma\tau_w$
0
0.05
0.1
0.15
0.2
k_P
ext.coil+rad.sensor
ext.coil+ext.pol.sensor
ext.coil+int.pol.sensor
int.coil+rad.sensor
int.coil+ext.pol.sensor
int.coil+int.pol.sensor

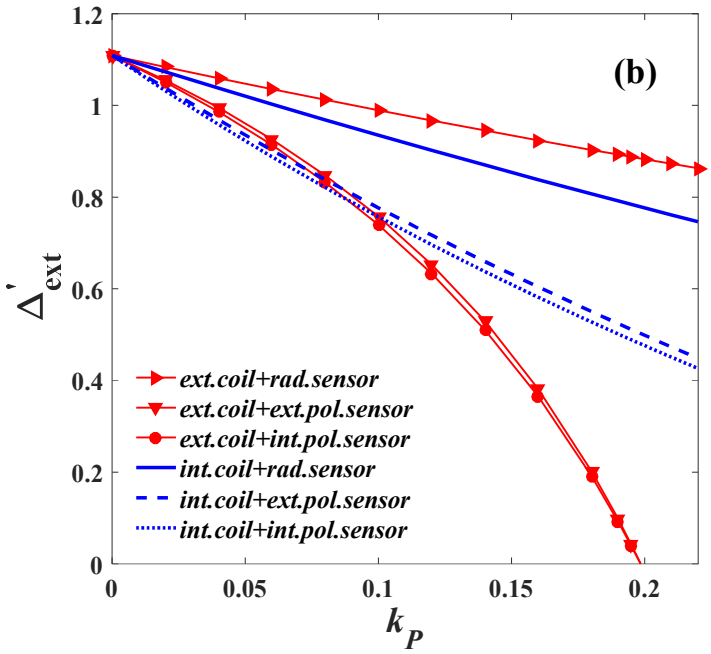
(b)
1.2
1
0.8
0.6
0.4
0.2
0
Δ'_{ext}
0
0.05
0.1
0.15
0.2
k_P
ext.coil+rad.sensor
ext.coil+ext.pol.sensor
ext.coil+int.pol.sensor
int.coil+rad.sensor
int.coil+ext.pol.sensor
int.coil+int.pol.sensor

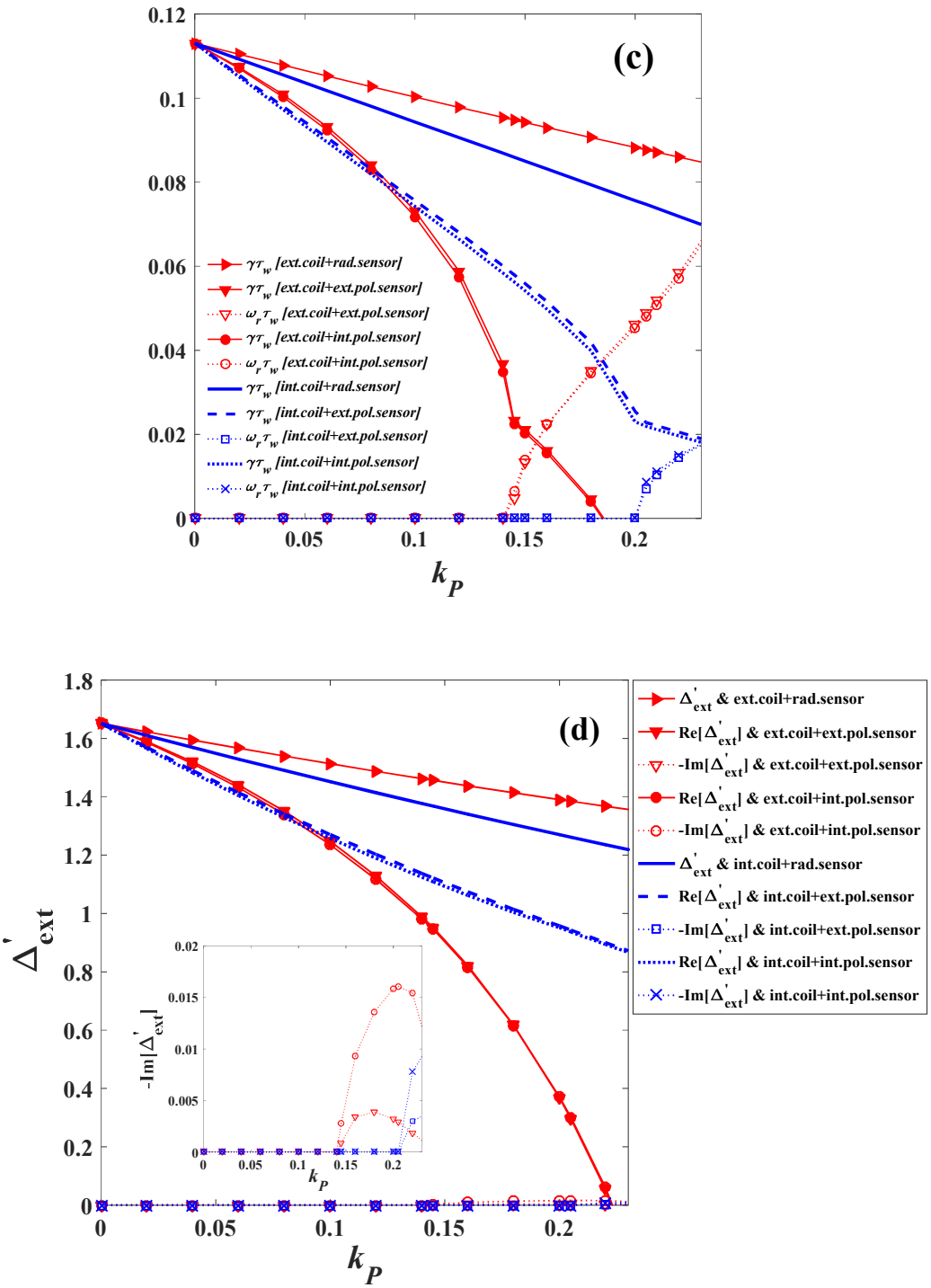

Fig. 5 Close-loop results for the n=1 RP-RWM, assuming equilibria with (a-b) vanishing pressure $\beta = 0$, and (c-d) finite pressure $\beta = 0.03$ with the GGJ included into the inner layer tearing index ($D_R = -0.0003$). Compared are results with various feedback coil configurations assuming proportional control. Plotted are (a,c) the mode growth rate, and (b,d) the external tearing index. The on-axis safety factor is fixed at

$q_0 = 1.05$.

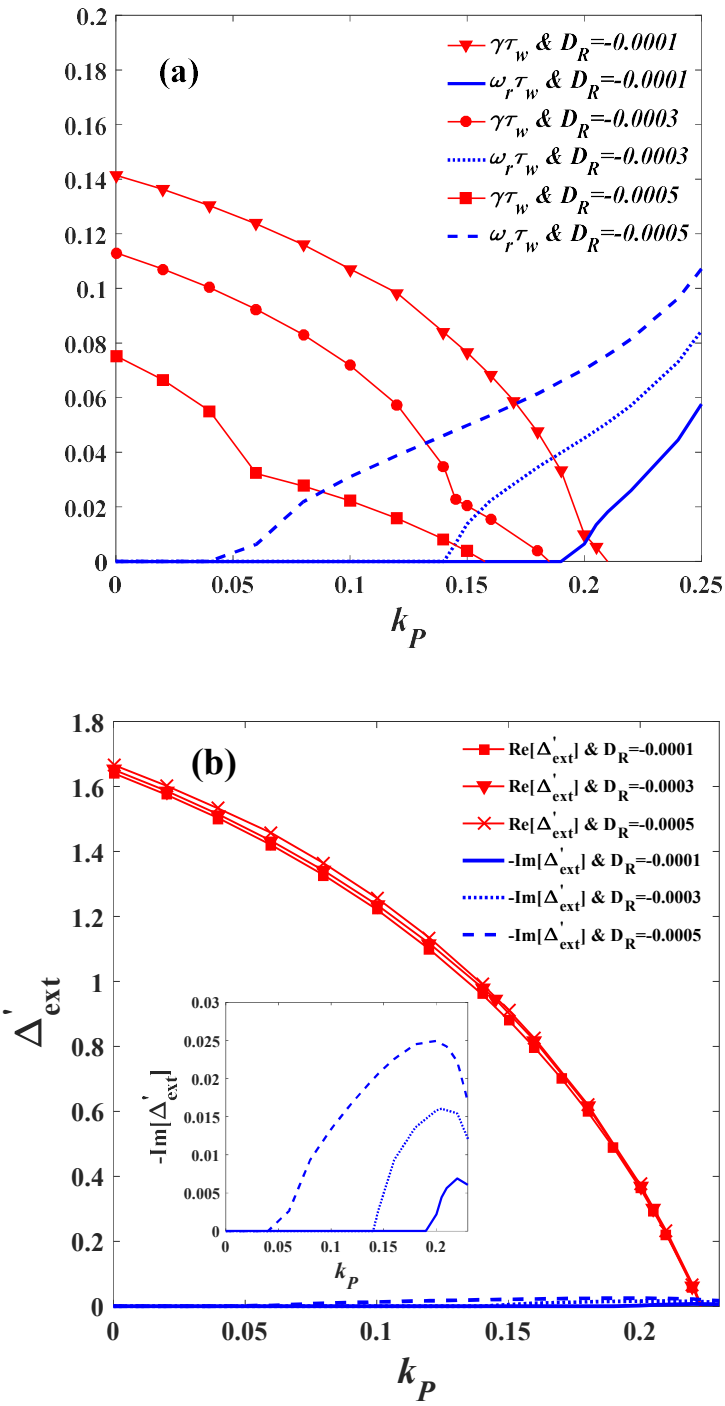

Fig. 6 Close-loop results for the n=1 RP-RWM for (a) the mode eigenvalues, and (b) the external tearing index, while scanning the proportional feedback gain and varying the value of the resistive interchange index. Considered is a plasma with finite equilibrium pressure ($\beta = 0.03$). Assumed is a control scheme with the external active coil and the internal poloidal sensor. The on-axis safety factor is fixed at $q_0 = 1.05$.

B. Feedback with PD-gain

We now solve Eq. (14) but with the external tearing index defined by expression (10). We fix the proportional gain at $k_P = 0.1$ and scan the derivative gain k_D. The results are presented in Fig. 7, without (a-b) or with (c-d) the GGJ effect. Note that the general trend remains similar between the two cases (with or without the GGJ effect). For the case with the GGJ effect (c-d), the proportional gain is chosen such that the close-loop eigenvalue is real at vanishing derivative gain. The latter, when introduced, does not yield finite mode frequency.

The feedback results with either external or internal poloidal sensors remain similar while scanning the derivative gain. This is largely because the mode growth is already weak at $k_P = 0.1$ and k_D =0. A weakly growing instability does not introduce large eddy current in the resistive wall. We also note that the derivative gain is stabilizing with all types of feedback coil configurations, including the combination of internal active coils and the radial sensor (albeit with very weak effect).

Similar to the case for the IP-RWM, the derivative action does not fully stabilize the RP-RWM. Both the mode growth rate and the external tearing index tend to saturate at large k_D values.

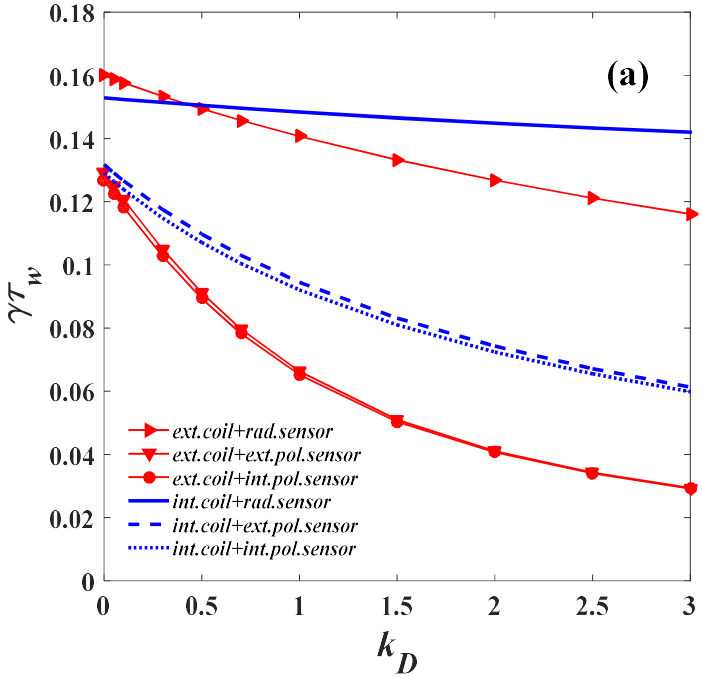
(a)
0.18
0.16
0.14
0.12
0.1
0.08
0.06
0.04
0.02
0
$\gamma\tau_w$
0
0.5
1
1.5
2
2.5
3
k_D
ext.coil+rad.sensor
ext.coil+ext.pol.sensor
ext.coil+int.pol.sensor
int.coil+rad.sensor
int.coil+ext.pol.sensor
int.coil+int.pol.sensor

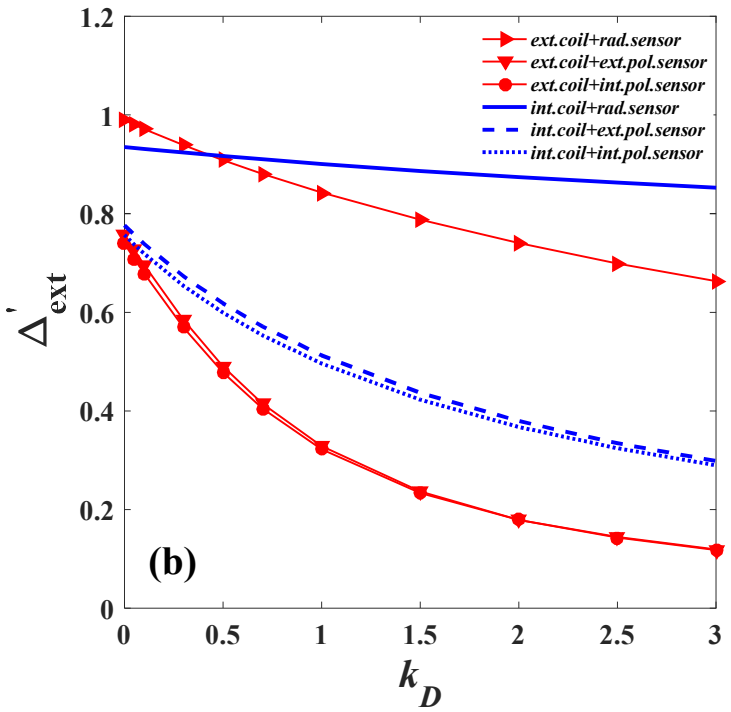
(b)
1.2
1
0.8
0.6
0.4
0.2
0
Δ'_{ext}
0
0.5
1
1.5
2
2.5
3
k_D
ext.coil+rad.sensor
ext.coil+ext.pol.sensor
ext.coil+int.pol.sensor
int.coil+rad.sensor
int.coil+ext.pol.sensor
int.coil+int.pol.sensor

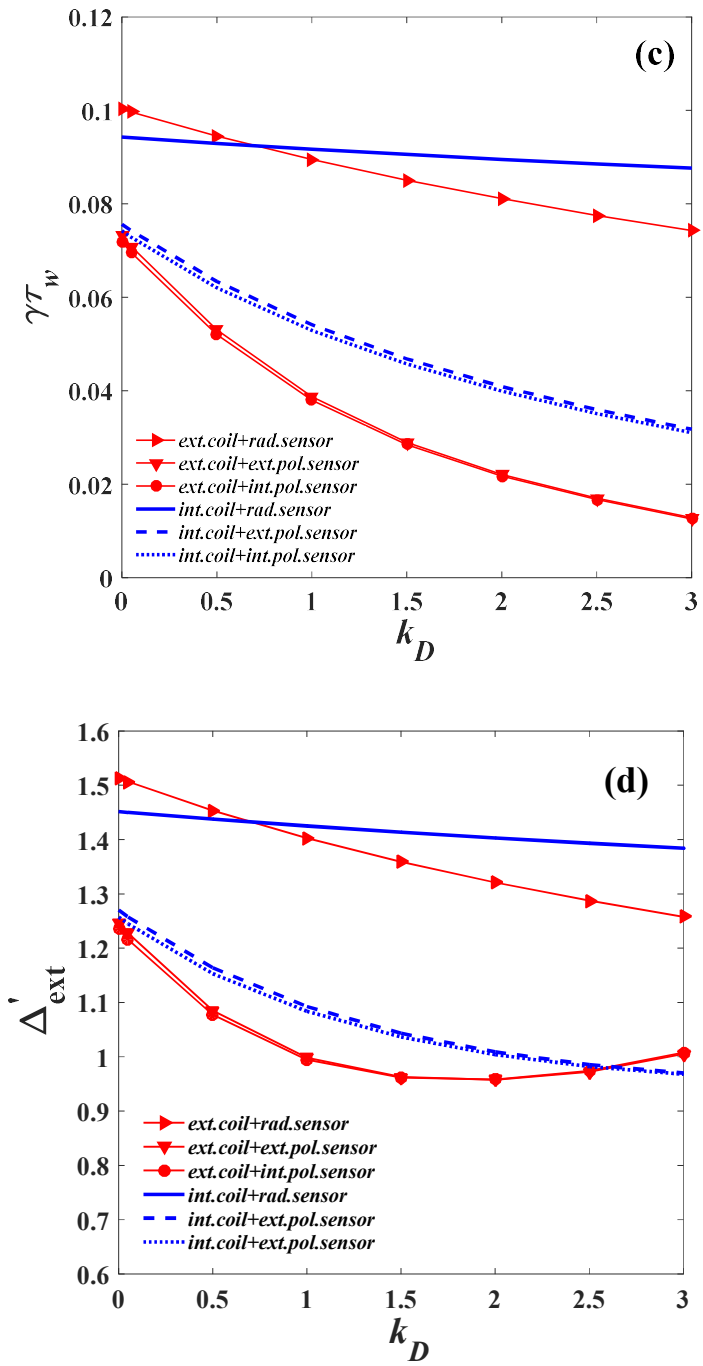

Fig. 7 Close-loop results for the n=1 RP-RWM, assuming equilibria with (a-b) vanishing pressure $\beta = 0$, and (c-d) finite pressure $\beta = 0.03$ with the GGJ included into the inner layer tearing index ($D_R = -0.0003$). Compared are results with various feedback coil configurations while scanning the derivative gain. The proportional gain is fixed at $k_P = 0.1$. Plotted are (a,c) the mode growth rate, and (b,d) the external tearing index. The on-axis safety factor is fixed at $q_0 = 1.05$.

V. Feedback control of RP-EK via modification of Δ'_{ext}

As the final step of investigation, we consider feedback stabilization of the RP-EK. Active control of the EK is normally not practically feasible due to the fast open-loop growth (in Alfvenic time scale). This is however not the case for the RP-EK, due to substantial reduction of the mode growth rate by the plasma resistivity, as shown in Fig. 2. We shall again consider P- and PD-control, with or without the GGJ physics in the inner layer. The basic plasma parameters remain the same as that in Sec. III, except for the on-axis safety factor $q_0 = 1.2$ and the equilibrium pressure $\beta = 0.05$. The other obvious difference is that the plasma inertia is now always retained in evaluating the external tearing index.

A. P-feedback

Figure 8 shows that feedback stabilization of the RP-EK is generally weak, due to weak modification of the external tearing index. The exception is the coil combination with external active coils and the internal or external poloidal sensor. However, as pointed out in Sec. III, the strong stabilization with external active coils should be viewed with caution, due to the artifact associated with the single harmonic approximation. Another observation is the large difference in the feedback results, between the internal and external poloidal sensors. This is due to much stronger instability (the open-loop growth rate of the

RP-EK is about one order of magnitude higher than that of the RP-RWM) which induces larger eddy currents in the resistive wall.

With external active coils, the two stability curves with internal and external poloidal sensors intersect at the feedback gain value of $k_P = 0.25$. This is not a co-incidence. Detailed analysis of the expression (8) for the external tearing index reveals that, at this gain value, or more generally at $k_P = 1/2m$, the parameter $\alpha_P = 1$ holds independent of the wall time, resulting in the same stabilization effect. For the special case of vanishing wall ($\tau_w = 0$), the difference in the definition between the internal and the external poloidal sensors naturally disappears.

Similar to the RP-RWM, inclusion of the GGJ effect results in a rotating RP-EK at large proportional gain ($k_P > 0.3$) and with external active coils (Fig. 8(c)). The corresponding external tearing index also becomes complex-valued, with large magnitude of $\mathrm{Im}(\Delta'_{\mathrm{ext}})$ in this case. The imaginary part of the outer tearing index is again primarily introduced by the wall eddy current induced perturbed energy dissipation, as discussed before. The transition from the real to complex eigenvalue depends on the value of k_P and D_R, as shown in Fig. 9. When the absolute value of D_R is sufficiently small (e.g. $D_R = -0.001$), the eigenvalue of the RP-EK and the value of the corresponding Δ'_{ext} are all real. In addition, for the range of k_P between 0 and 0.25, Δ'_{ext} remains real independent of the choice for the D_R value.

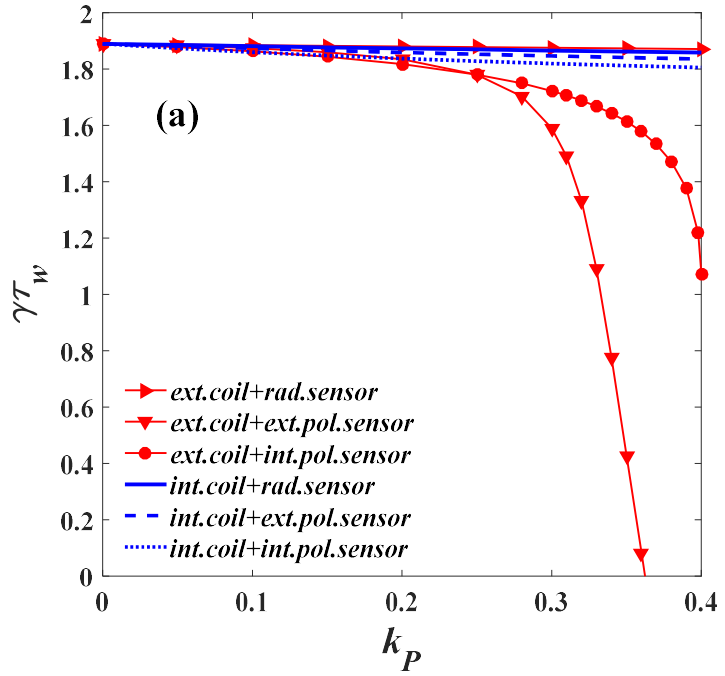
(a)
$\gamma\tau_w$
k_P
ext.coil+rad.sensor
ext.coil+ext.pol.sensor
ext.coil+int.pol.sensor
int.coil+rad.sensor
int.coil+ext.pol.sensor
int.coil+int.pol.sensor

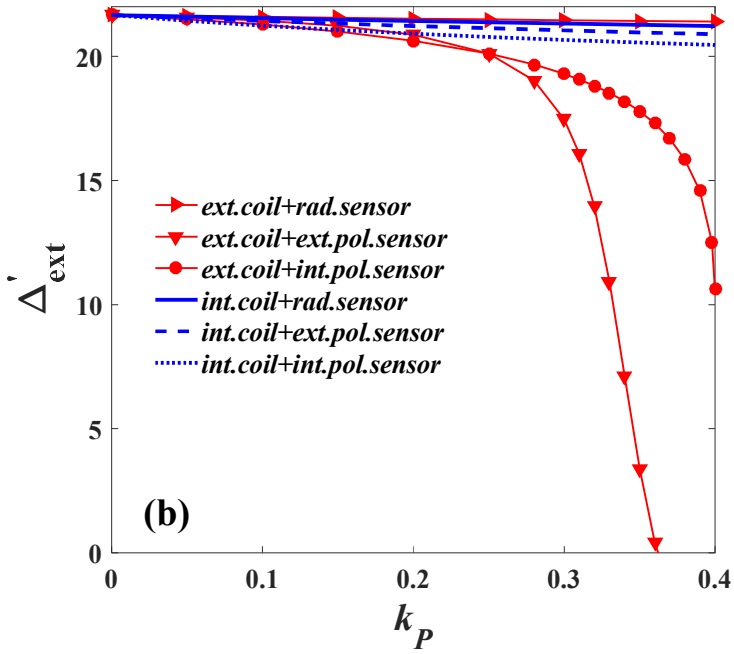
(b)
Δ'_{ext}
k_P
ext.coil+rad.sensor
ext.coil+ext.pol.sensor
ext.coil+int.pol.sensor
int.coil+rad.sensor
int.coil+ext.pol.sensor
int.coil+int.pol.sensor

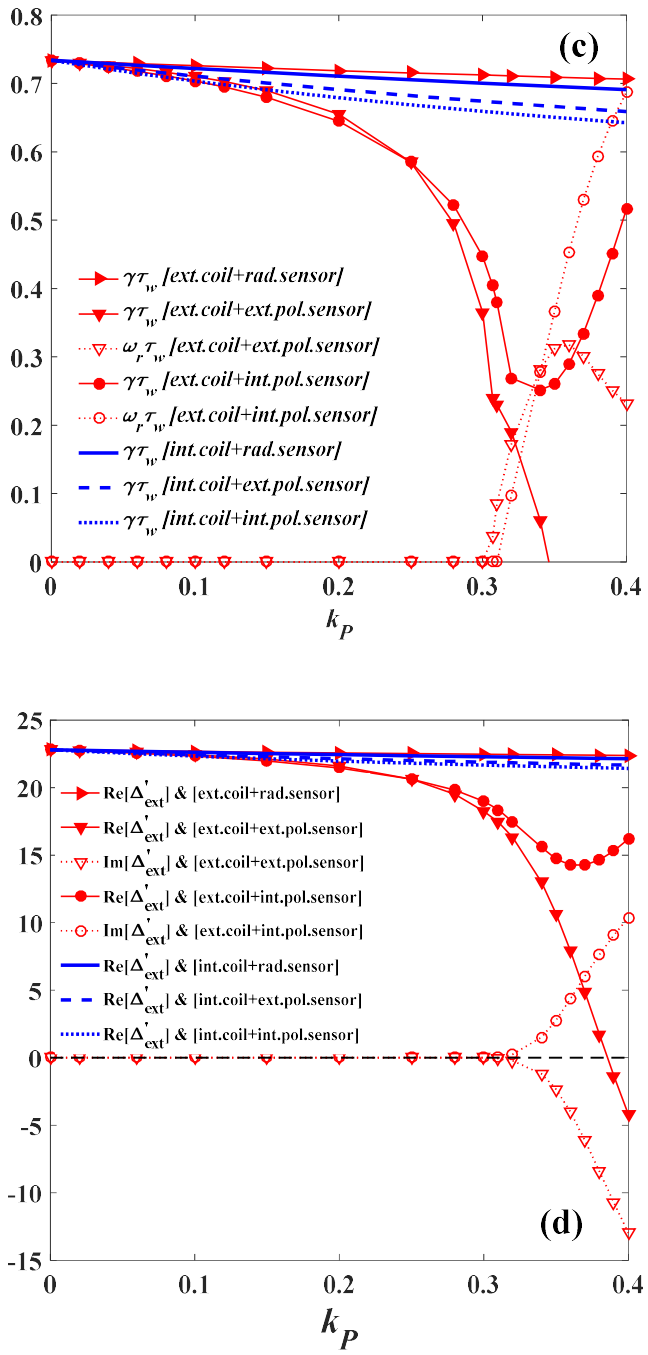

Fig. 8 Close-loop results for the n=1 RP-EK, assuming equilibria with (a-b) vanishing pressure $\beta = 0$, and (c-d) finite pressure $\beta = 0.05$ with the GGJ included into the inner layer tearing index ($D_R = -0.01$). Compared are results with various feedback coil configurations assuming proportional control. Plotted are (a,c) the mode growth rate, and (b,d) the external tearing index. The on-axis safety factor is fixed at $q_0 = 1.2$.

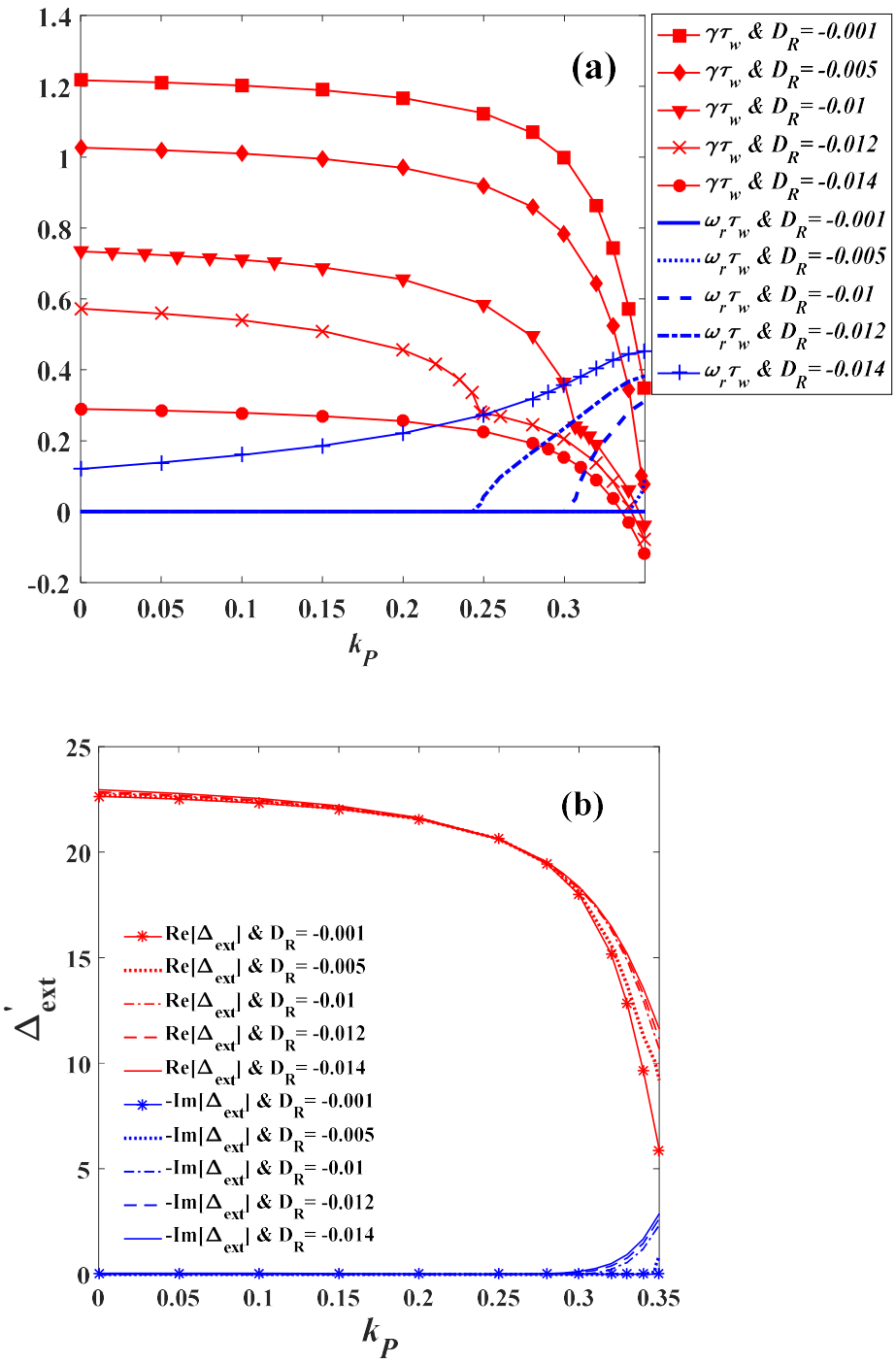

Fig. 9 Close-loop results for the n=1 RP-EK for (a) the mode eigenvalues and (b) the complex external tearing index, while scanning the proportional feedback gain and varying the value of the resistive interchange index $D_R = -0.001 \sim -0.014$. Considered is a plasma with finite equilibrium pressure ($\beta = 0.05$). Assumed is a control scheme with the external active coil and the external poloidal sensor. The on-axis safety factor is fixed at $q_0 = 1.2$.

B. PD-feedback

Figure 10 reports feedback results by numerically solving Eq. (14), which links expression (10) with (12) or (13), while scanning the derivative gain k_D at fixed proportional gain of $k_P = 0.25$. Among various combinations of the active and sensor coils, the external active coil, combined with poloidal sensors, stands out as the most effective one in reducing the mode growth rate by the derivative action. An interesting new observation here is that, for the RP-EK, the derivative action at large gain value can also introduce complex close-loop eigenvalue (Fig. 10(c)) and complex Δ'_{ext} (Fig. 10(d)). Moreover, the real part of Δ'_{ext} increases with increasing the derivative (at large gain values). This is in contrast to the monotonic decrease of the mode growth rate with increasing k_D.

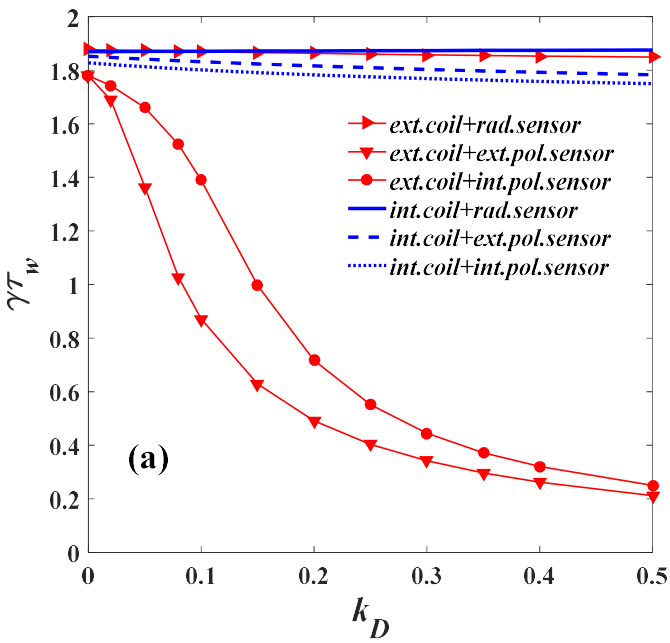

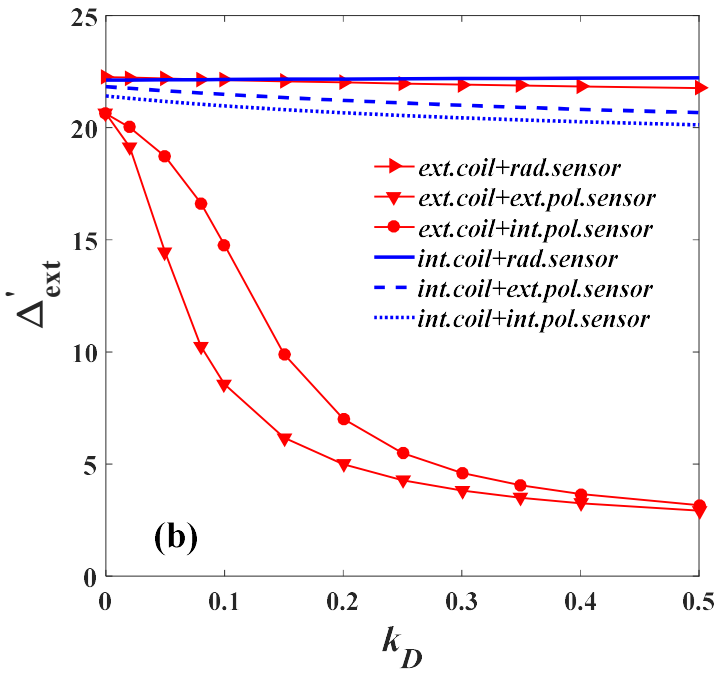
25
20
15
10
5
0
0
0.1
0.2
0.3
0.4
0.5
Δ'_{ext}
k_D
(b)
ext.coil+rad.sensor
ext.coil+ext.pol.sensor
ext.coil+int.pol.sensor
int.coil+rad.sensor
int.coil+ext.pol.sensor
int.coil+int.pol.sensor

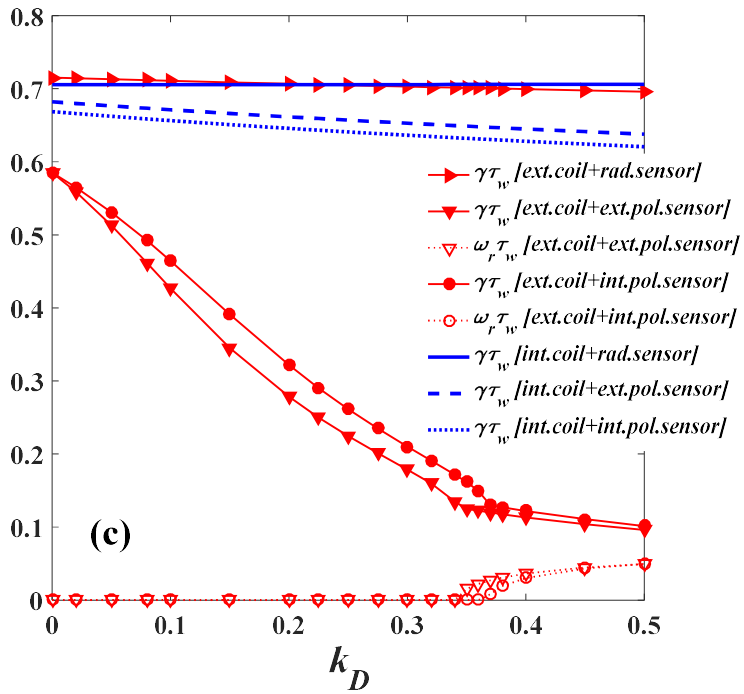
0.8
0.7
0.6
0.5
0.4
0.3
0.2
0.1
0
0
0.1
0.2
0.3
0.4
0.5
k_D
(c)
$\gamma\tau_w$ [ext.coil+rad.sensor]
$\gamma\tau_w$ [ext.coil+ext.pol.sensor]
$\omega_r\tau_w$ [ext.coil+ext.pol.sensor]
$\gamma\tau_w$ [ext.coil+int.pol.sensor]
$\omega_r\tau_w$ [ext.coil+int.pol.sensor]
$\gamma\tau_w$ [int.coil+rad.sensor]
$\gamma\tau_w$ [int.coil+ext.pol.sensor]
$\gamma\tau_w$ [int.coil+int.pol.sensor]

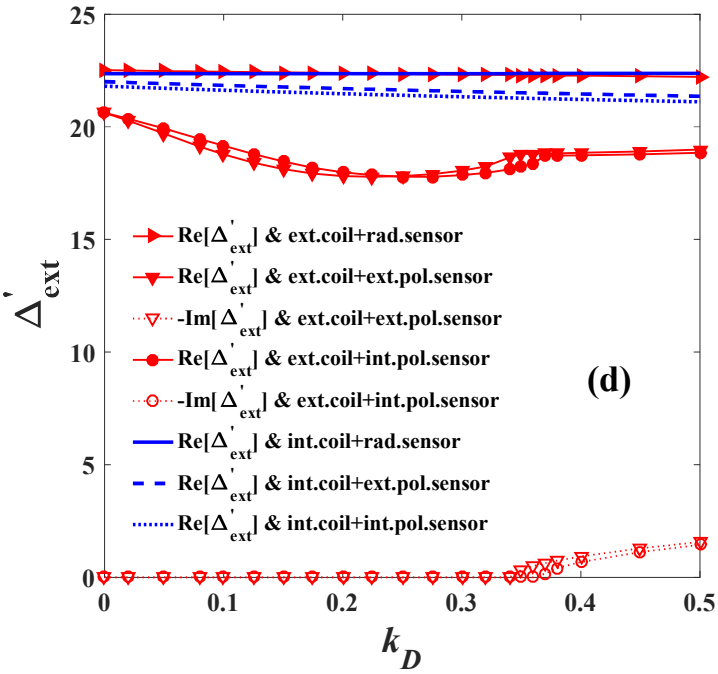

Fig. 10 Close-loop results for the n=1 RP-EK, assuming equilibria with (a-b) vanishing pressure $\beta = 0$, and (c-d) finite pressure $\beta = 0.05$ with the GGJ included into the inner layer tearing index ($D_R = -0.01$). Compared are results with various feedback coil configurations while scanning the derivative gain. The proportional gain is fixed at $k_P = 0.25$. Plotted are (a,c) the mode eigenvalue, and (b,d) the complex external tearing index. The on-axis safety factor is fixed at $q_0 = 1.2$.

In the presence of the GGJ effect, the derivative gain induced complex mode eigenvalue (and Δ'_{ext}) appears to be qualitatively different from that induced by the proportional action. This is demonstrated in Fig. 11, where we compare the P- and PD-control of the RP-EK, while scanning the D_R value. The feedback scheme combines the external active coil and the external poloidal sensor. Apparently, with increasing D_R (towards the negative value), the growth rate of the RP-EK decreases

(Fig. 11(a)). The close-loop eigenvalue becomes complex at certain value of D_R. This transition occurs for both the open-loop and close-loop with either P- or PD-feedback, though at different D_R values.

The real part of the corresponding external tearing index Δ'_{ext} is independent of the resistive interchange index in the open-loop or close-loop with P-feedback. This implies that the RP-EK is controlled by the proportional feedback via modification of Δ'_{ext}, not via changing the inner layer physics. On the other hand, the same derivative action does result in different Δ'_{ext} while varying the D_R value. Fig. 11(b) shows that, under the same derivative action, the external tearing index increases with increasing D_R (towards negative value), despite the fact that the growth rate of the RP-EK decreases. The effect of the derivative feedback action is thus non-trivial in terms on modifying the external tearing index. On the other hand, the P-feedback, with either $k_P = 0.25$ or $k_P = 0.3$, produces constant Δ'_{ext} values independent of D_R.

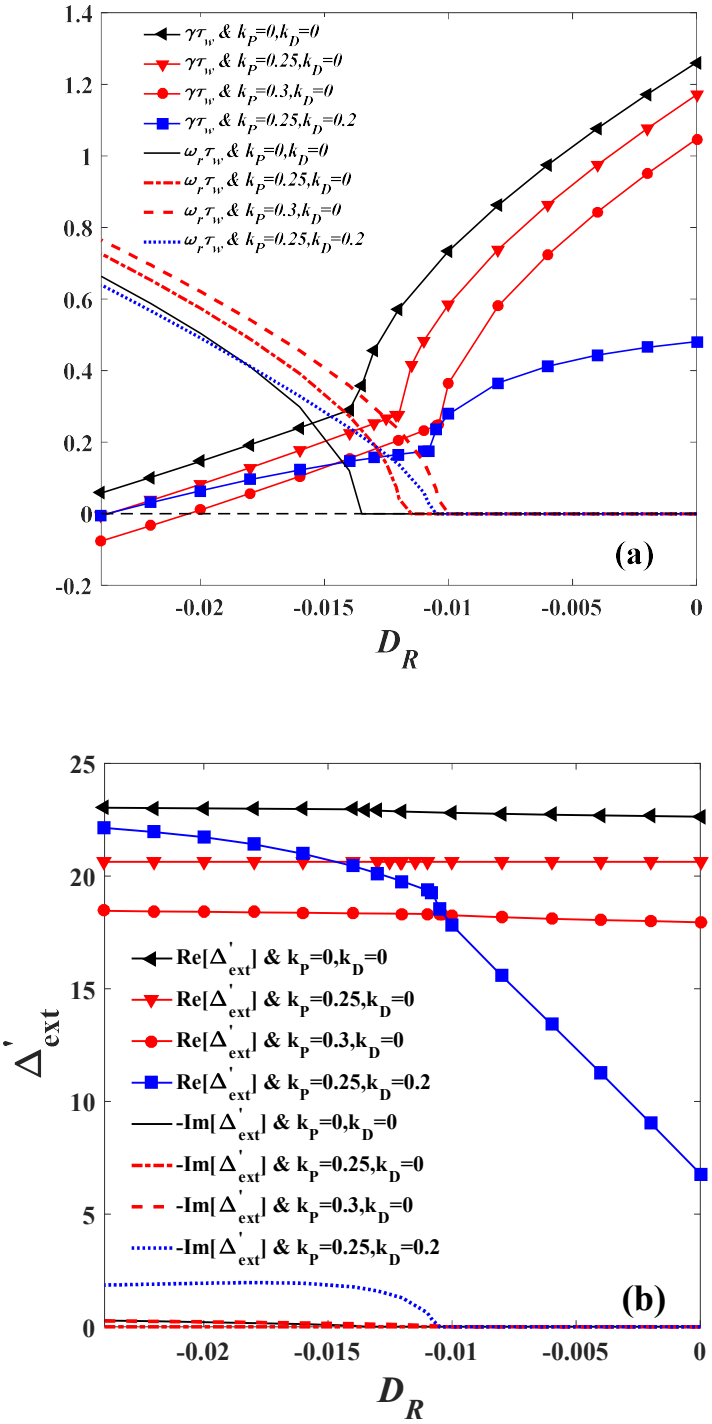

Fig. 11 Open-loop and close-loop results for the n=1 RP-EK, for (a) the mode eigenvalue, (b) the complex external tearing index, while scanning the resistive interchange index. Compared also are the results with proportional feedback and with PD-feedback. Considered is a plasma with finite equilibrium pressure $\beta = 0.05$. Assumed is the feedback configuration with the external active coil and the external poloidal sensor. The on-axis safety factor is fixed at $q_0 = 1.2$.

VI. Conclusion

Based on an analytic model, we have carried out systematic investigation on feedback control of the RP-RWM and RP-EK via the matching method (Eq. (14)). The same method is also applied to study the IP-RWM as a special case, i.e. with vanishing inner layer tearing index at the mode rational surface. A key merit of the matching approach is that feedback modification of the external tearing index can be quantified, by inserting the self-consistently calculated eigenvalue from the close-loop Eq. (14) back into expression (8) or (10). For the RP-RWM and RP-EK, the instability is controlled mainly via feedback modification of the external tearing index, as demonstrated in this work.

Assuming six feedback coil configurations combining different types of active and sensor coils, we calculate modification of Δ'_{ext} by the P- and PD-control systems, and map out the results in parameter spaces involving the proportional gain k_P, the derivative gain k_D, and the resistive interchange index D_R. We find that increasing either the proportional or derivative gain generally reduces Δ'_{ext} and stabilizes the RP-RWM or RP-EK, with all six feedback configurations.

Feedback generally affects the external tearing index Δ'_{ext} independent of the inner layer physics, implying that feedback stabilizes the RP-RWM or RP-EK primarily via modification of the solution in the outer ideal region. One exception is the case where either sufficiently

large GGJ effect or strong control action produces a rotating instability in the static plasma. The close-loop external tearing index then becomes complex-valued, due to the perturbed magnetic energy dissipation in the outer region, associated with the eddy current flowing in the resistive wall. The plasma inertia (again from the outer region) in principle plays a similar role as the wall eddy current, but the effect on Δ'_{ext} is several orders of magnitude weaker during feedback stabilization of the RP-RWM and RP-EK. For the latter, the inertia effect is already significantly reduced by plasma resistive damping in the open-loop.

With single harmonic approximation, which is the constraint for the matching method, we find that the combination of external active coils and poloidal sensors often outperforms the other feedback configurations at large feedback gain. This counter-intuitive result is explained as lack of (non-resonant) poloidal harmonics for proper description of the feedback coil geometry. This is confirmed by including multiple poloidal harmonics in the alternative control model based on the plasma response transfer function (the PRM model), which has previously been developed to study feedback control of the IP-RWM.

Acknowledgments

This work was funded by National Natural Science Foundation of China (NSFC) (Grant Nos. 11905067, 11847219 and 11905022), and the China

Postdoctoral Science Foundation under Grant No.2019M652931. Chongqing Basic Research and Frontier Exploration Project in 2019 (Chongqing Natural Science Foundation: cstc2019jcyj-msxmX0567).

Appendix A

This Appendix lists simplified versions for the open-loop and close-loop growth rates of the IP-RWM in special cases. The open-loop growth rate of the IP-RWM is derived from Eq. (6)

$$\gamma_{nf}\tau_w = -2m\frac{1-(m-nq_0)}{1-(r_0/r_w)^{2m}-(m-nq_0)}. \tag{A.1}$$

For the plasma with vanishing equilibrium pressure ($\beta = 0$), the close-loop growth rate with the P-controller can be straightforwardly obtained for the IP-RWM, assuming various combinations of the active and sensor coil types

$$\gamma\tau_w = \begin{cases} -2mk_P + C_1 & ext.coil + rad.sensor \\ (-C_2mk_P + C_1)/(1-2mk_P) & ext.coil + ext.pol.sensor \\ -C_2mk_P + C_1 & ext.coil + int.pol.sensor \\ -C_3k_P + C_1 & int.coil + rad.sensor \\ -C_3mk_P + C_1 & int.coil + ext.pol.sensor \\ (-C_3mk_P + C_1)/(1+C_3k_P) & int.coil + int.pol.sensor \end{cases} \tag{A.2}$$

where $C_1 = \gamma_{nf}\tau_w$, $C_2 = -2m\frac{1-(m-nq_0)+(r_0/r_w)^{2m}}{1-(m-nq_0)-(r_0/r_w)^{2m}}$ and

$C_3 = 2m\dfrac{1-(m-nq_0)-(r_0/r_f)^{2m}}{1-(m-nq_0)-(r_0/r_w)^{2m}}$ are all positive constants.

Assuming the combination of internal active coils and the radial sensor, the close-loop growth rate with a PD-control is calculated as

$$\gamma\tau_w = \frac{-C_3k_P + C_1}{-C_4k_D + 1} \tag{A.3}$$

where $C_4 = -\dfrac{2m[1-(m-nq_0)]-(r_0/r_f)^{2m}}{1-(m-nq_0)-(r_0/r_w)^{2m}}$ is also a positive constant.

Appendix B

This Appendix exploits the PRM approach for feedback control of the IP-RWM, in order to compare with the matching approach adopted in the main part of this work, and to explain certain counter-intuitive results obtained with the matching approach. Specifically, Sec. III finds that the combination of the external active coil and the poloidal sensor provides more efficient control at large proportional gain, than the internal active coil.

Below we repeat the key steps in deriving the PRM model.[23-25] For each poloidal harmonic *m*, the corresponding transfer function $M^m(s)$, from the control current to the sensor signal, is obtained for the same equilibrium (with vanishing pressure) as specified in Sec. II.

(i) The perturbed radial field component b_r satisfies the ideal MHD force balance condition at the plasma boundary surface $r = a +$

$$\left.\frac{rb_r'}{b_r}\right|_{a+} = C \tag{B.1}$$

where C is a constant independent of feedback.

(ii) The wall equation (thin wall is assumed)

$$\left.\frac{r\left[b_r'\right]}{b_r}\right|_{r_w} = 2s \tag{B.2}$$

where $s = \gamma\tau_w$ is the growth rate of the RWM with feedback.

(iii) The total field in various vacuum regions outside the plasma can be written as the sum of contributions from the plasma, the wall and the active coil currents

$$b_r = b_r^p\left(\frac{r}{a}\right)^{sgn(a-r)\mu-1} + b_r^w\left(\frac{r}{r_w}\right)^{sgn(r_w-r)\mu-1} + b_r^f\left(\frac{r}{r_f}\right)^{sgn(r_f-r)\mu-1} \tag{B.3}$$

The above three conditions yield a relation

$$\frac{\mu-1-C}{\mu+1+C}\left(\frac{a}{r_w}\right)^{2\mu} = -\frac{\gamma_{nf}\tau_w+\mu}{\gamma_{nf}\tau_w} \tag{B.4}$$

where $\gamma_{nf}\tau_w = -\mu\dfrac{1\mp(m-nq_0)}{1\mp(m-nq_0)-(r_0/r_w)^{2\mu}}$ is the growth rate of the ideal external kink mode, with $\mu = |m|$ and $\mp$ stands for $-sgn(m)$.

Define the open-loop transfer function for the radial and poloidal sensors as

$$M_r^m(s) \equiv \frac{b_r^s}{b_r^f} \tag{B.5}$$

and

$$M_\theta^m(s) \equiv \frac{jb_\theta^s\big|_{r_s}}{b_r^f}, \quad b_\theta^s\big|_{r_s} = \frac{j}{m}\left(rb_r^s\right)'\Big|_{r_s} \tag{B.6}$$

respectively, where b_r^s is the total radial field at the sensor position,

which is assumed to be the wall radial position. Considering various combinations of the active and sensor coil types, the transfer functions for the radial and poloidal sensors are obtained by expressing b_r^p, b_r^w and b_r^s via b_r^f, yielding

$$M_r^m(s)=\begin{cases}\dfrac{\alpha}{s-\gamma_{nf}\tau_w} & (r_f<r_w)\\[2ex] \dfrac{\beta}{s-\gamma_{nf}\tau_w} & (r_w<r_f)\end{cases} \tag{B.7}$$

$$M_\theta^m(s)=\begin{cases}\dfrac{\mu+2s}{m(s-\gamma_{nf}\tau_w)}\alpha & (r_f<r_s<r_w)\\[2ex] \dfrac{\mu}{m(s-\gamma_{nf}\tau_w)}\alpha & (r_f<r_w<r_s)\\[2ex] \dfrac{\mu\lambda}{m(s-\gamma_{nf}\tau_w)} & (r_s<r_w<r_f)\\[2ex] \dfrac{\mu(\lambda-2\kappa s)}{m(s-\gamma_{nf}\tau_w)} & (r_w<r_s<r_f)\end{cases} \tag{B.8}$$

where $\begin{cases}\alpha=\mu(r_w/r_f)^{\mu-1}+\gamma_{nf}\tau_w\left[(r_w/r_f)^{\mu-1}-(r_w/r_f)^{-\mu-1}\right]\\ \beta=\mu(r_w/r_f)^{\mu-1}\\ \lambda=2\gamma_{nf}\tau_w(r_w/r_f)^{\mu-1}+\mu(r_w/r_f)^{\mu-1}\\ \kappa=(r_w/r_f)^{\mu-1}\end{cases}$.

The open-loop total transfer functions[24] for different poloidal harmonics are coupled via a window-pane representation of the active coils and the point-wise sensor signal (for either the radial or poloidal sensors), resulting in a total transfer function of

$$P(s)=\sum_m M^m(s)f_m\,exp(jm\theta_c)exp(jm\theta_s)$$

where θ_c (θ_s) is the poloidal angle of the center of the active (sensor)

coil locations, and f_m is the geometrical coupling factor

$$f_m = \frac{m}{2\mu}\frac{sin(m\theta_f)}{sin\,\theta_f}\frac{r_w^2 + r_f^2 - 2r_w r_f\, cos\,\theta_f}{r_f^2}$$

where θ_f being the half-width of the poloidal coverage by the active coils.

With a proportional controller and feedback gain G, the close-loop eigenvalue is determined by the solution of the characteristic equation

$$1 + GP(s) = 0 \tag{B.9}$$

Taking the single-m poloidal harmonic approximation, the close-loop eigenvalue is readily calculated

$$s = \begin{cases} \gamma_{nf}\tau_w - H\beta & ext.coil + rad.sensor \\ \dfrac{m\gamma_{nf}\tau_w - H\lambda\mu}{m - 2H\kappa\mu} & ext.coil + ext.pol.sensor \\ \dfrac{m\gamma_{nf}\tau_w - H\lambda\mu}{m} & ext.coil + int.pol.sensor \\ \gamma_{nf}\tau_w - H\alpha & int.coil + rad.sensor \\ \dfrac{m\gamma_{nf}\tau_w - H\alpha\mu}{m} & int.coil + ext.pol.sensor \\ \dfrac{m\gamma_{nf}\tau_w - H\alpha\mu}{m + 2H\alpha} & int.coil + int.pol.sensor \end{cases} \tag{B.10}$$

where $H = f_m G$ for the single row of active coils and sensor coils located at the outboard mid-plane ($\theta_c = 0$ and $\theta_s = 0$). It is evident that the PRM approach yields the same feedback result, (B.10), as that from the matching approach from the IP-RWM (setting expression (8) $= 0$), i.e. (A.2) from Appendix A. The difference in the coefficients comes from different definition of the control signals.

The above expression (B.10) (or equivalently expression (A.2))

shows that a P-control with the internal active coil and the internal poloidal sensor provides more stabilization than that of the external active coil ($\frac{m\gamma_{nf}\tau_w - H\lambda\mu}{m} > \frac{m\gamma_{nf}\tau_w - H\alpha\mu}{m+2H\alpha}$), if the feedback gain is sufficiently small $0 < H < \frac{\gamma_{nf}\tau_w + 1}{\lambda} - \frac{1}{\alpha}$. However, at large feedback gain $H > \frac{\gamma_{nf}\tau_w + 1}{\lambda} - \frac{1}{\alpha}$, the external active coil becomes more effective ($\frac{m\gamma_{nf}\tau_w - H\lambda\mu}{m} < \frac{m\gamma_{nf}\tau_w - H\alpha\mu}{m+2H\alpha}$). These results are also plotted in Fig. B(a).

On the other hand, we can also numerically solve Eq. (B.9), by including two harmonics ($m = \pm 2$) or even multiple harmonics ($m = -10 \sim 10$) in the transfer function $P(s)$. The calculated close-loop growth rates for the IP-RWM are plotted in Fig. B(b) and (c), respectively. In both cases, we find that the internal active coil provides stronger stabilization to the mode than the external active coil, independent of the proportional feedback gain value.

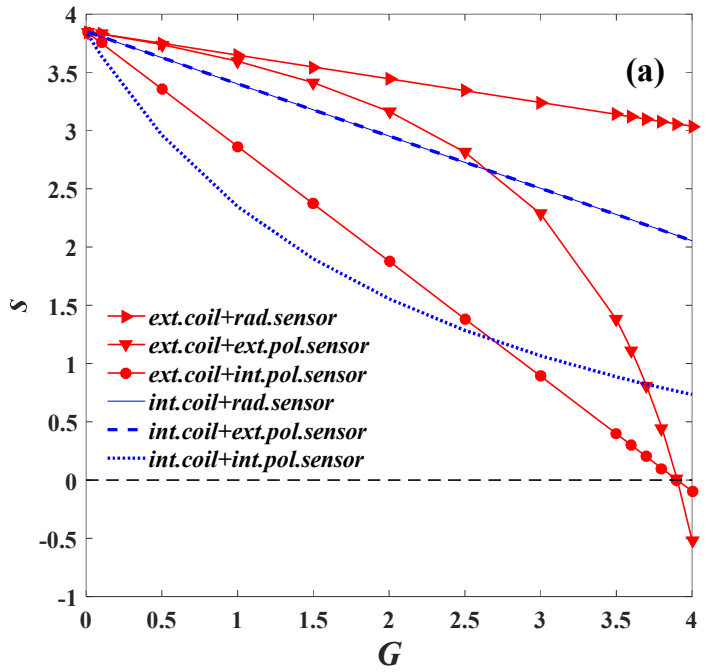
(a)
S
G
ext.coil+rad.sensor
ext.coil+ext.pol.sensor
ext.coil+int.pol.sensor
int.coil+rad.sensor
int.coil+ext.pol.sensor
int.coil+int.pol.sensor

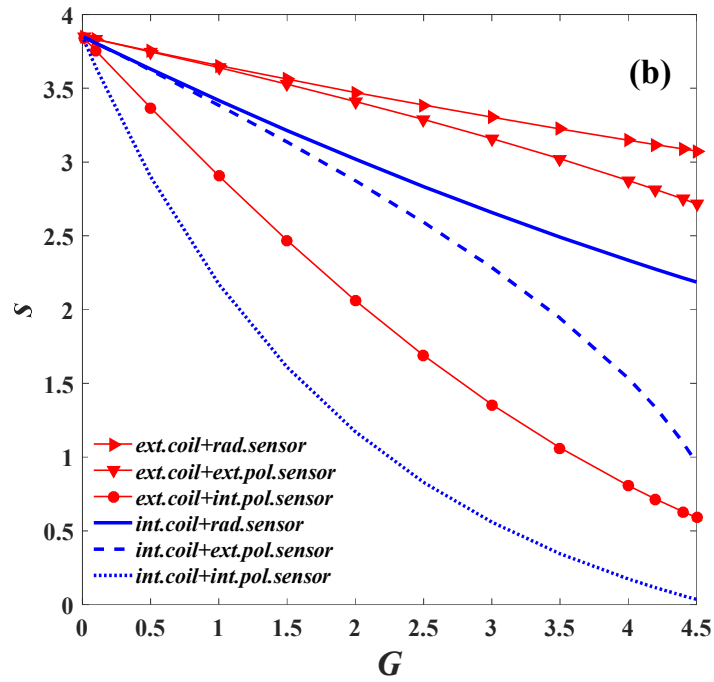
(b)
S
G
ext.coil+rad.sensor
ext.coil+ext.pol.sensor
ext.coil+int.pol.sensor
int.coil+rad.sensor
int.coil+ext.pol.sensor
int.coil+int.pol.sensor

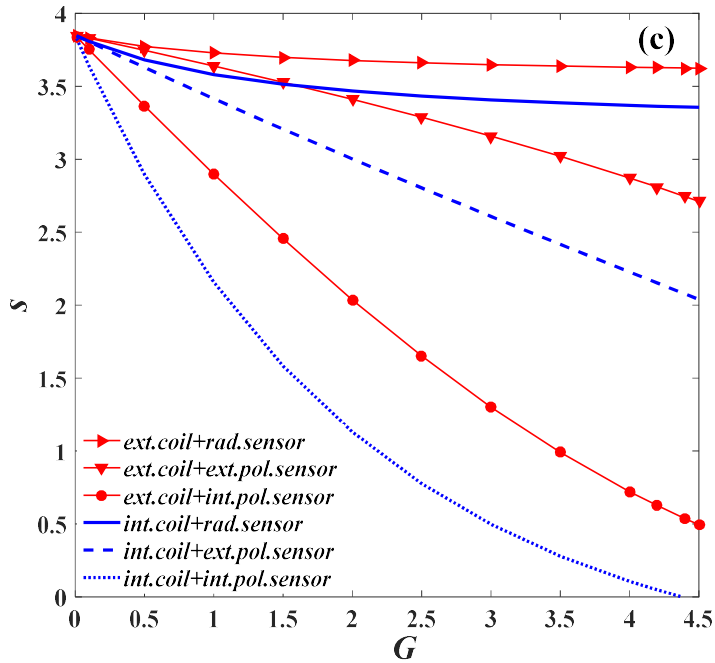

Fig. B The growth rates of the $n=1$ IP-RWM versus the feedback gain, assuming various combinations of the active and sensor coil types. The poloidal coverage by the active coil is fixed $\theta_f = \pi/9$. (a) single-m poloidal harmonic ($m=2$), (b) two poloidal harmonics ($m=\pm 2$) and (c) multiple poloidal harmonics ($m=-10\sim 10$) are considered in the transfer function $P(s)$, respectively.

Reference

[1] T. C. Hender, J. C. Wesley, J. Bialek, A. Bondeson, A. H. Boozer, R. J. Buttery, A. Garofalo, T. P. Goodman, R. S. Granetz, Y. Gribov, O. Gruber, M. Gryaznevich, G. Giruzzi, S. G€unter, N. Hayashi, P. Helander, C. C. Hegna, D. F. Howell, D. A. Humphreys, G. T. A. Huysmans, A. W. Hyatt, A. Isayama, S. C. Jardin, Y. Kawano, A. Kellman, C. Kessel, H. R. Koslowski, R. J. L. Haye, E. Lazzaro, Y. Q. Liu, V. Lukash, J. Manickam, S. Medvedev, V. Mertens, S. V. Mirnov, Y. Nakamura, G. Navratil, M. Okabayashi, T. Ozeki, R. Paccagnella, G. Pautasso, F. Porcelli, V. D. Pustovitov, V. Riccardo, M. Sato, O. Sauter, M. J. Schaffer, M. Shimada, P. Sonato, E. J. Strait, M. Sugihara, M. Takechi, A. D. Turnbull, E. Westerhof, D. G. Whyte, R. Yoshino, H. Zohm, and the ITPA MHD, Disruption and Magnetic Control Topical Group, Nucl. Fusion 47, S128 (2007).

[2] M. S. Chu and M. Okabayashi, Plasma Phys. Controlled Fusion 52, 123001 (2010).

[3] F. Troyon, R. Gruber. H. Saurenmann, S. Semenzato, and S. Succi, Plasma Phys. Controlled Fusion 26, 209 (1984).

[4] A. Bondeson and D. Ward, Phys. Rev. Lett. 72, 2709 (1994).

[5] M. S. Chu, J. M. Greene, T. H. Jensen, R. L. Miller, A. Bondeson, R. W. Johnson, and M. E. Mauel, Phys. Plasmas 2, 2236 (1995).
[6] R. Betti and J. P. Freidberg, Phys. Rev. Lett. 74, 2949 (1995).
[7] R. Fitzpatrick and A. Y. Aydemir, Nucl. Fusion 36, 11 (1996).
[8] J. R. Drake, P. R. Brunsell, D. Yadikin, M. Cecconello, J. A. Malmberg, D. Gregoratto, R. Paccagnella, T. Bolzonella, G. Manduchi, L. Marrelli, S. Ortolani, G. Spizzo, P. Zanca, A. Bondeson, and Y. Q. Liu, Nucl. Fusion 45, 557 (2005).
[9] V. D. Pustovitov, Nucl. Fusion 55, 033008 (2015).
[10] J. M. Finn, Phys. Plasmas 2, 198 (1995).
[11] J. M. Finn, Phys. Plasmas 2, 3782 (1995).
[12] A. Bondeson and H. X. Xie, Phys. Plasmas 4, 2081 (1997).
[13] Y. L. He, Y. Q. Liu, Y. Liu, G. Z. Hao, and A. K. Wang, Phys. Rev. Lett. 113, 175001 (2014).
[14] Y. L. He, Y. Q. Liu, Y. Liu, C. Liu, G. L. Xia, A. K. Wang, G. Z. Hao, L. Li, and S. Y. Cui, Physics of Plasmas 23, 012506 (2016).
[15] S. X. Yang, Y. Q. Liu, G. Z. Hao, Z. X. Wang, Y. L. He, H. D. He, A. K. Wang, and M. Xu, Phys. Plasmas 25, 012125 (2018).
[16] Y. Q. Liu and A. Bondeson, Phys. Rev. Lett. 84 907 (2000).
[17] S. Sabbagh, R. Bell, J. Menard, D. Gates, A. Sontag, J. Bialek, B. LeBlanc, F. Levinton, K. Tritz and H. Yuh, Phys.Rev. Lett. 97 045004 (2006).
[18] Y. Q. Liu, M. S. Chu, I. T. Chapman and T. C. Hender, Phys. Plasmas 15 112503 (2008)
[19] G. L. Xia, Y. Liu and Y. Q. Liu, Plasma Phys. Control. Fusion 56 095009 (2014).
[20] G. L. Xia, Y. Q. Liu, C.J. Ham, S. Wang, L. Li, G.Y. Zheng, J. X. Li, N. Zhang, X. Bai, G.Q. Dong and The HL-2M Team, Nucl. Fusion 59 016017 (2019).
[21] S. Wang, Y.Q. Liu, G.Y. Zheng, X.M. Song, G.Z. Hao, G.L. Xia, L. Li, B. Li, N. Zhang, G.Q. Dong and X. Bai, Nucl. Fusion 59 096021 (2019).
[22] J. M. Finn, Phys. Plasmas 13, 082504 (2006).
[23] A. Bondeson, Y. Q. Liu D. Gregoratto, Y. Gribov and V. D. Pustovitov, Nucl. Fusion 42, 768 (2002).
[24] Y. Q. Liu, Plasma Phys. Control. Fusion 48, 969 (2006).
[25] J. Ren, Y. Q. Liu, Y. Liu and S. Y. Medvedev, Nucl. Fusion 58, 126017 (2018).
[26] A. Bondeson, H. X. Xie, Phys. Plasmas 4, 2081 (1997).
[27] H. P. Furth, J. Killeen, and M. N. Rosenbluth, Phys. Fluids 6, 459 (1963).
[28] Y Q. Liu, R. J. Hastie, and T. C. Hender, Phys. Plasmas 19, 092510 (2012).
[29] A. H. Glasser, J. M. Greene, and J. L. Johnson, Phys. Fluids 18, 875 (1975).
[30] W. A. Newcomb, Ann. Phys. (N.Y.) 10, 232 (1960).
[31] B. Coppi, R. Galvao, R. Pellat, M. N. Rosenbluth, and P. H. Rutherford, Fiz. Plazmy 2, 961 (1976) [Sov. J. Plasma Phys. 2, 533 (1976)].
[32] A. H. Glasser, J. M. Greene, and J. L. Johnson, Phys. Fluids 19, 567 (1976).
[33] Y. Q. Liu, J. W. Connor, S. C. Cowley, C. J. Ham, R. J. Hastie, and T. C. Hender, Phys. Plasmas 19, 072509 (2012).
[34] R. Fitzpatrick, T. H. Jensen, Phys. Plasmas 3, 2641 (1996).
[35] M. Okabyashi, N. Pomphrey and R.E. Hatcher, Nucl. Fusion 38, 1607 (1998).